MID-AMERICA TRANSPORTATION CENTER

Report # MATC-UNL: 004-55

Final Report

WBS: 27-1121-0005-004-55

Application of Microfiber Reinforcement to Weak Soils for Alternative Road Stabilization Strategy

Jonwan Eun, PhD, PE
Associate Professor
Department of Civil and Environmental Engineering
University of Nebraska-Lincoln

Seunghee Kim, PhD, PE
Associate Professor

Laith Ibdah
Graduate Research Assistant

Kenaz Owusu
Graduate Research Assistant

2024

A Cooperative Research Project sponsored by
U.S. Department of Transportation- Office of the Assistant Secretary for Research and Technology

The contents of this report reflect the views of the authors, who are responsible for the facts and the accuracy of the information presented herein. This document is disseminated in the interest of information exchange. The report is funded, partially or entirely, by a grant from the U.S. Department of Transportation's University Transportation Centers Program. However, the U.S. Government assumes no liability for the contents or use thereof.

Application of Microfiber Reinforcement to Weak Soils for Alternative Road Stabilization Strategy

Jongwan Eun, Ph.D., P.E.
PI
Associate Professor
Civil and Environmental Engineering Department

Laith Ibdah
Graduate Research Assistant
Civil and Environmental Engineering Department

Seunghee Kim, Ph.D., P.E.
Co-PI Associate Professor
Civil and Environmental Engineering Department

Kenaz Owusu
Graduate Research Assistant
Civil and Environmental Engineering Department

A Report on Research Sponsored by

Mid-America Transportation Center

University of Nebraska–Lincoln

September 2024

Technical Report Documentation Page

1. Report No. 25-1121-0005-004-55	2. Government Accession No.	3. Recipient's Catalog No.
4. Title and Subtitle Application of Microfiber Reinforcement to Weak Soils for Alternative Road Stabilization Strategy		5. Report Date September 2024
		6. Performing Organization Code
7. Author(s) Jongwan Eun, Seunghee Kim, Laith Ibdah, Kenaz Owusu		8. Performing Organization Report No. 25-1121-0005-004-55
9. Performing Organization Name and Address University of Nebraska-Lincoln Department of Civil and Environmental Engineering Nebraska Hall, 900 N 16th St Lincoln, NE 68508		10. Work Unit No. (TRAIS)
		11. Contract or Grant No. 69A3551747107
12. Sponsoring Agency Name and Address Office of the Assistant Secretary for Research and Technology 1200 New Jersey Ave., SE Washington, D.C. 20590		13. Type of Report and Period Covered June 2021 to Aug 2024
		14. Sponsoring Agency Code MATC TRB RiP No. 91994-104
15. Supplementary Notes		

16. Abstract
This report explores the application of microfiber reinforcement as an alternative strategy for stabilizing weak subgrade soils, particularly in roadway construction. The study evaluates the effectiveness of microfiber reinforcement by conducting a comprehensive literature review and performing a series of experimental tests, including Unconfined Compressive Strength (UCS) tests and Large-Scale Track Wheel (LSTW) tests. The experiments were designed to assess the impact of varying microfiber contents (0% to 1% by weight) on the strength, stiffness, and overall performance of Nebraska soils. The findings indicate that microfiber reinforcement can significantly enhance the mechanical properties of weak soils, with the UCS results showing an increase in strength and the LSTW tests demonstrating improved resistance to deformation.

17. Key Words soil stabilization, micro fiber reinforcement, laboratory test	18. Distribution Statement		
19. Security Classif. (of this report) Unclassified	20. Security Classif. (of this page) Unclassified	21. No. of Pages 88	22. Price

Table of Contents

List of Figures

List of Tables

Disclaimer

The contents of this report reflect the views of the authors, who are responsible for the facts and the accuracy of the information presented herein. The contents do not necessarily reflect the official views or policies neither of the Nebraska Department of Transportation nor the University of Nebraska-Lincoln. This report does not constitute a standard, specification, or regulation. Trade or manufacturers' names, which may appear in this report, are cited only because they are considered essential to the objectives of the report.

The United States (U.S.) government and the State of Nebraska do not endorse products or manufacturers. This material is based upon work supported by the Federal Highway Administration under SPR-P1(see your contract for this #. Any opinions, findings and conclusions or recommendations expressed in this publication are those of the author(s) and do not necessarily reflect the views of the Federal Highway Administration."

Abstract

This study investigated the application of microfiber reinforcement as an alternative strategy for stabilizing weak subgrade soils, particularly in roadway construction. The study evaluated the effectiveness of microfiber reinforcement by conducting a comprehensive literature review and performing a series of experimental tests, including Unconfined Compressive Strength (UCS) tests and Large-Scale Track Wheel (LSTW) tests. The experiments were designed to assess the impact of varying microfiber contents (0% to 1% by weight) on the strength, stiffness, and overall performance of selected Nebraska soils. The findings indicate that microfiber reinforcement can significantly enhance the mechanical properties of weak soils, with the UCS results showing an increase in strength and the LSTW tests demonstrating improved resistance to deformation.

Chapter 1 Introduction

1.1 Introduction

The concept of Fiber Reinforced Soil (FRS) has historical roots in ancient construction practices, where natural fibers, such as straw, were integrated into materials like mud roofs and clay bricks to enhance their structural integrity. These early applications demonstrated the efficacy, cost-effectiveness, and straightforwardness of incorporating fibers to improve construction materials. In contemporary engineering, FRS involves the integration of synthetic fibers, such as polypropylene, with soil to enhance its shear and tensile resistance (Divya et al. 2014; Go et al. 2015).

Chemical stabilization is a well-known technique used to enhance soil strength and durability through the addition of various chemical additives such as lime, cement, and fly ash. However, chemical stabilization poses significant environmental concerns, including increased greenhouse gas emissions. Additionally, there are limitations to using chemical stabilization, such as its ineffectiveness on frozen soil, soil with low silica content, and its applicability to certain soil types (Hensley et al. 2007). In contrast, FRS presents a crucial, sustainable, and cost-effective alternative, providing substantial improvements in soil properties without the adverse environmental impacts associated with traditional chemical methods (Mirzababaei, et al. 1988; Zheng, et al. 2021).

In recent years, there has been a growing interest among researchers worldwide in FRS. Both synthetic fibers, such as polypropylene, and natural fibers have been employed to enhance the mechanical and physical properties of soil (Maher and Ho 1994). This approach treats the soil as a composite material, with the random distribution of fibers significantly increasing its tensile and shear strength. FRS has been a beneficial option to control swelling and shrinkage durably and

economically in many geotechnical applications, such as foundation soils by generating frictional and tensile resistance between clay particles and the fiber filaments that distribute external forces (Tang et al. 2016; Li and Zornberg 2019). Accordingly, FRS could be promising for enhancing the performance of the subgrade as an alternative to chemical stabilization. This study goals are:

1. A comprehensive review of existing literature on microfiber reinforcement applications in weak soils, focusing particularly on subgrade stabilization practices across different states.
2. Evaluation of geotechnical properties, including strength and stiffness, of Nebraska soils mixed with varying percentages (0% to 1% by weight) of fiber reinforcement.
3. Comparative analysis of the performance between subgrade and fiber-reinforced subgrade soils using the Large-Scale Track Wheel (LSTW) test.
4. Identification of site-specific applicability and cost-effectiveness of microfiber-reinforced subgrade solutions.

Aligned with the focus areas of the Mid-America Transportation Center, this project aims to enhance road safety and improve roadway serviceability through innovative approaches to subgrade stabilization.

1.2 Problem Statement

The objective of this study is to evaluate the effectiveness of microfiber reinforcement on reducing swelling/shrinkage potentials and controlling the plasticity of weak soils as an alternative road stabilization strategy. Lime stabilization does not work well for less pozzolanic reactive soils (Hensley et al. 2007). Microfiber reinforcement as tensile inclusions in weak soils has been a beneficial option to control swelling and shrinkage durably and economically in many geotechnical applications, such as foundation soils by generating frictional and tensile resistance between clay particles and the fiber filaments that distribute external forces (Divya et al. 2014;

Gao et al. 2015). Accordingly, microfiber reinforcement could be promising for enhancing the performance of the subgrade as an alternative to lime stabilization. However, currently, there are no well-defined provisions regarding microfiber reinforcement design for weak soils. Furthermore, the mechanisms underlying the mechanical behavior of these interfacial surfaces between the reinforcement and soil particles are not fully understood yet. Overall, there is a lack of studies that assess the performance of microfiber reinforced soils quantitatively in many states as well as Nebraska. Thus, a systematic study is needed to help to facilitate the usage of fiber-reinforced subgrade stabilization.

1.3 Objectives of the Study

The objectives of this study are:

1. To evaluate the effectiveness of microfiber reinforcement as an alternative stabilization strategy for controlling problematic subgrade soils.
2. To modify and conduct multi-scale experimental studies to evaluate the fundamental geotechnical properties of fiber-reinforced soils. In particular, the study will include a large-scale track wheel (LSTW) test to explore, investigate, and refine the understanding of the mechanical behavior and performance of microfiber-reinforced soils.

Chapter 2 Literature Review

2.1 Practical Case on the Application of Fiber in Other States

2.1.1 Iowa

White et al. (2013) conducted a project on Cement Stabilization with Fiber Reinforcement of Subbase at the Central Iowa Expo Site in Boone, Iowa. In collaboration with its research partners, the Iowa Department of Transportation (Iowa DOT) designed comparative pavement foundation test sections. The project was constructed between May and July of 2012, covering 4.8 miles of roadway with sixteen 700-foot-long test sections. The primary objectives of the project were to create a testing area for long-term performance monitoring and to expand the range of stabilization technologies considered for future pavement foundation designs, thereby optimizing the pavement system. Two types of fibers were used for reinforcement: black polypropylene (PP) and white monofilament polypropylene (MF-PP). The mixing rates for fiber and cement were set at 0.4% and 5%, respectively. The summary of results indicated that the stiffness and strength of the stabilized soil were achieved after three months. On average, the performance of the two types of fibers combined with cement was similar. However, the modulus of the subbase layer stabilized with fibers alone (without Portland cement) showed lower values at all three testing intervals compared to the sections stabilized with both Portland cement and fibers.

2.1.2 Oklahoma

Hatami et al. (2018) developed comprehensive guidelines for the application of Fiber Reinforced Soil (FRS) in highway construction, with a particular focus on its use in the repair of shallow slope failures in Oklahoma. Their study includes two extensive case studies, which demonstrate the application of FRS. These case studies represent some of the largest

implementations of FRS technology in the United States, underscoring the method's practicality and effectiveness.

The authors emphasized that the field implementation of FRS is relatively straightforward, as it parallels the processes involved in similar technologies, such as chemical stabilization. The study found that FRS does not require proprietary equipment; instead, it can be effectively utilized with standard construction equipment and techniques. This ease of integration not only minimizes the learning curve for construction personnel but also offers significant cost savings. The ability to employ local workforces and equipment further contributes to the economic and practical advantages of using FRS, as evidenced by the successful outcomes of the case studies presented in the report. As expected, the integration of fiber-reinforced soil, particularly with problematic subgrade materials, will be straightforward for the reasons mentioned previously.

2.1.3 Texas

Gregory (2006), in his doctoral dissertation, presented case history projects for the application of fiber-reinforced soil (FRS) stabilization. One significant project discussed is the President George Bush Turnpike (PGBT) in the Dallas, Texas area. This multi-segment, six-lane toll road was constructed over five years to alleviate the increasing vehicle traffic in the region as shown in **Figure 2.1**. The PGBT is located within the Eagle Ford Shale geologic formation, characterized by expansive clays prone to widespread shallow slope failures a few years after embankment construction, particularly for slopes of 15 feet in height. In response to these challenges, Gregory (2006) recommended the use of FRS as a preventive maintenance measure. He specifically advised applying FRS to the top six feet of the side slopes to significantly reduce the potential for shallow slope failures. The recommendation targeted slopes taller than 15.5 feet

and steeper than a slope ratio of 4:1. The application rate was set at six pounds per cubic yard, resulting in approximately 520,000 pounds of FRS being applied to the project.

Gregory further provided recommendations regarding the broader application of FRS in similar projects. He identified FRS as particularly effective in mitigating shallow slope failure conditions, where the failure surface zone is about 12 feet or less in depth. Additionally, he suggested that FRS could serve as secondary reinforcement in conjunction with geogrids, which are used as primary reinforcement for deeper slope failure conditions. He also recommended considering FRS for general use as veneer reinforcement in all new slopes with the potential for shallow slides, especially in highway embankment slopes that are difficult to repair or maintain. Beyond highway applications, FRS shows potential for use in landfill soil cover stabilization, as reinforcement in soil veneer over lightweight geofoam fill, and as key-trench fill.

Figure 1.1 Mixing and spreading fiber with soil in PGBT highway project (modified from Gregory 2006).

2.2 Practical Cases on the Application of Fiber Reinforcement in Roadways in Foreign Countries

Several studies have investigated the use of fiber reinforcement to improve the strength and stability of various subgrade soils, with promising results across different materials and environmental conditions. Sujatha et al. (2020) explored the reinforcement of lean clay soil using Alkali Resistant (AR) Glass Fiber and Electronic Grade (E) Glass Fiber, aiming to enhance soil strength and improve its suitability as a subgrade material. Their study demonstrated that the random inclusion of glass fibers significantly improved the unconfined compressive strength (UCS) and energy absorption capacity of the soil, with AR glass fiber outperforming E glass fiber across all tested proportions. Notably, the study found that the optimum fiber content was 0.75%, which led to substantial increases in the California Bearing Ratio (CBR) and a reduction in pavement design thickness.

Similarly, Rabab'ah et al. (2020) investigated the use of glass fibers as random reinforcement in expansive subgrade soils. The study focused on enhancing the soil's strength and stiffness for pavement applications, particularly in reducing the swell potential of expansive soils. The results confirmed that the inclusion of glass fibers notably improved the UCS, Indirect Tensile Strength (ITS), and stiffness of the soil, while also reducing its swelling characteristics. This enhancement in performance was directly proportional to the fiber content, suggesting that glass fiber reinforcement is an effective method for stabilizing expansive subgrade soils and can lead to reductions in pavement design thickness, similar to the findings of Sujatha et al.

Building on these findings, Madrid et al. (2024) conducted a study on the effectiveness of fiber incorporation in expansive clayey subgrade soils, using natural Ichu fiber and polypropylene fiber. Their research revealed that the addition of Ichu fibers significantly enhanced the UCS and resilient modulus (Mr) of the clayey soil, with the resilient modulus of fiber-reinforced soil being

at least 50% higher than that of non-reinforced soil. The study further found that a relatively low content of 0.25% polypropylene fiber was sufficient to double the resilient modulus, indicating that even small amounts of fiber reinforcement can have a profound impact on the mechanical behavior of expansive subgrade soils.

Chapter 3 Materials and Methods

3.1 Materials

3.1.1 Soil Type - Clay

The clay soil selected for this study was obtained from a site south of the US-75 at Plattsmouth (**Figure 3.1**, **Figure 3.2** and **Figure 3.3**). This is one of the common soil subgrade types found in Nebraska. Preliminary tests were conducted to find the soil characteristics and were performed following ASTM guidelines. Results from the soil characterization can be seen in **Table 3.1**. The maximum density obtained was 105 Ibs/ft^3 with an optimum moisture content of 18%. The soil-properties for the clay soil can be seen in **Table 3.1**. **Figure 3.4** shows the grain size distribution of the collected clay soil. The clay soil was classified as A-7-6 and CL based on the AASHTO and Unified soil classification system.

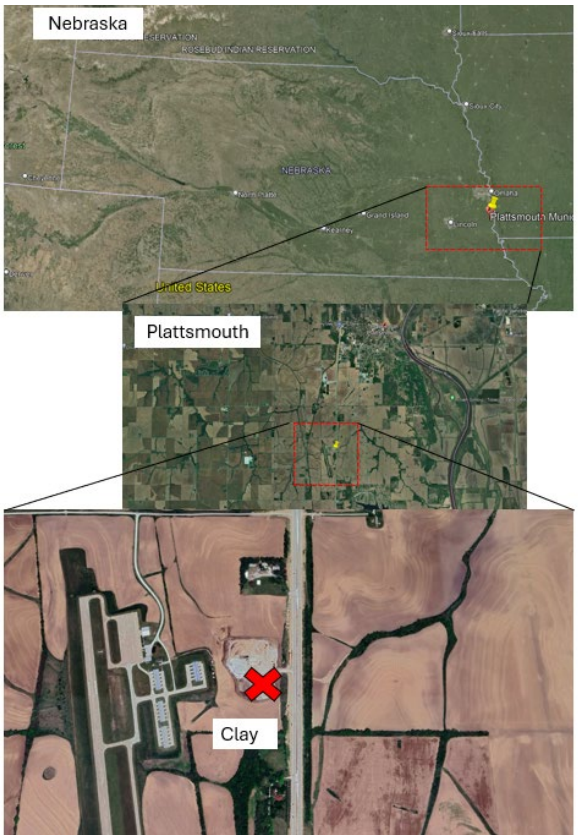

Figure 3.1 Location of clay collection area.

Figure 3.2 Soil excavation at Plattsmouth site

Figure 3.3 Clay soil at Plattsmouth site

Table 3.1 Properties of the clay.

Soil Type	Clay
Property	Value
Liquid Limit (%)	43
Plastic Limit (%)	24
Plasticity Index	19
Optimum Moisture Content (%)	18
Maximum Dry Density (Ibs/ft^3)	105
AASHTO Classification	A-7-6
UCS Classification	CL
Specific Gravity (G_s)	2.75

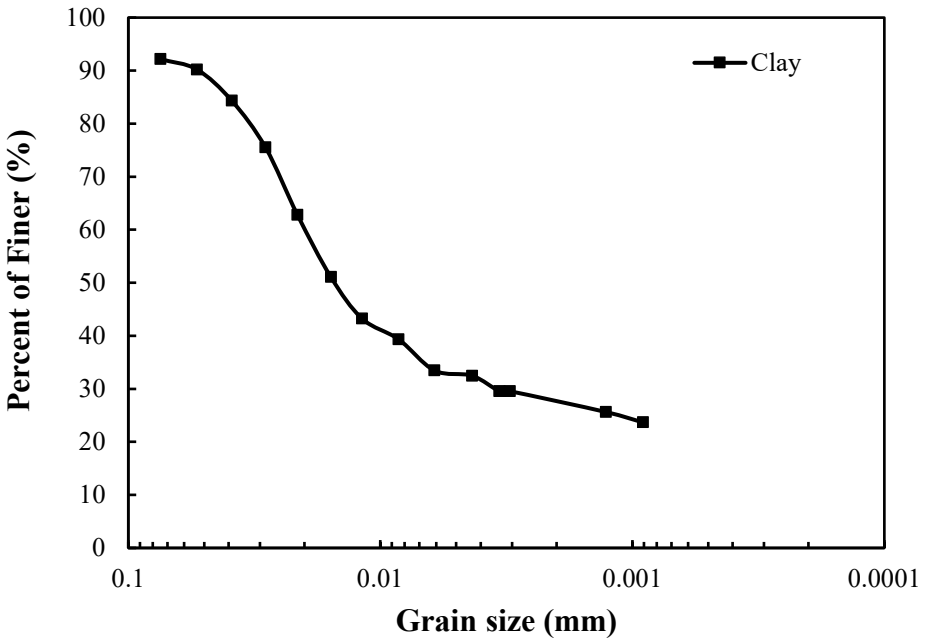

Figure 3.4 Grain size distribution graph for clay

3.1.2 Soil Type - Sand

Sand used for this study was obtained from a site south of the Platte River and Highway 50, as shown in **Figure 3.5**. Preliminary tests were conducted to obtain the soil characteristics and were performed following ASTM guidelines. Results from the soil characterization can be seen in **Table 3.2**.

Figure 3.6 shows the grain size distribution of the collected sand. The sand was medium-grained and between poor to well-graded with few fines. Sand was classified at A-1-b according to the AASHTO classification system.

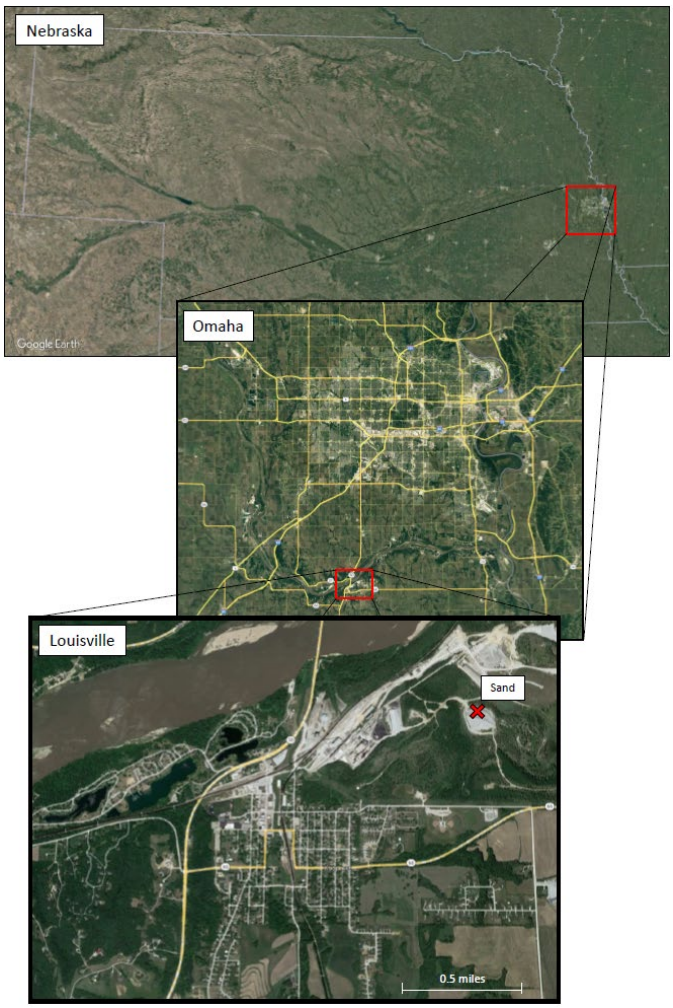

Figure 3.5 Location of clay collection area.

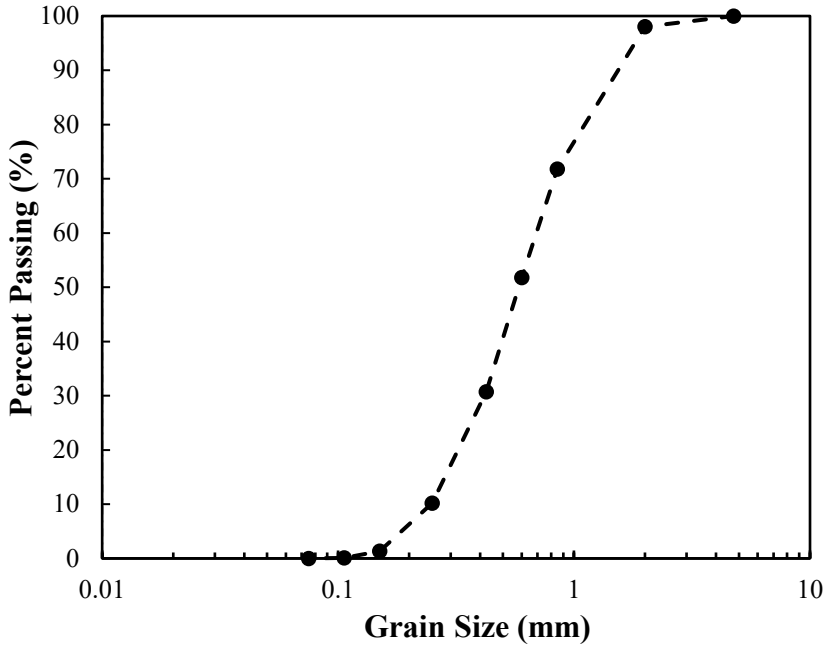

Figure 3.6 Grain size distribution graph for sand

Table 3.2 Properties of the sand.

Property	**Value**
D_{60}	0.69
D_{30}	0.41
D_{10}	0.22
Uniformity Coefficient (C_u)	3.14
Coefficient of Curvature (C_c)	1.11
AASHTO Classification	A-1-b
Specific Gravity (G_s)	2.65

3.1.3 Fiber

Fiber is a commonly used synthetic material for soil reinforcement. Polypropylene fiber was chosen for this study (see **Figure 3.7**). Polypropylene fiber, known for its high intensity monofilament made through advanced production technology, effectively controls microcracks

caused by shrinkage and temperature changes in concrete or mortar. This fiber was selected to evaluate the performance with soil application mainly for soil reinforcement. The properties of the fiber used for this study are highlighted in **Table 3.3**.

Table 3.3 Properties of Fiber

Property Raw Material	Polypropylene Fiber type monofilament
Cross-Section shape	Trefoil
Length (mm)	19
Moisture (%)	3 Max
Elastic Modulus (Mpa)	>3500
Elongation (%)	5-10
Tensile strength (Mpa)	≥500
Elongation at breaking(%)	≥15
Melting point(°C)	160-180
Acid-base resistance property(%)	≥94.4

Figure 3.7 Polypropylene fiber

3.2 Unconfined Compressive Strength (UCS) Test Program

3.2.1 UCS Apparatus Set-up

The Instron 68TM-50 was used for unconfined compressive strength (UCS) testing (see **Figure 3.8**). This device is a compact and versatile device, designed for a wide range of mechanical testing applications. It has a 11250 Ibf (50kN) force capacity. The load application and measurement are highly precise, with an accuracy of ±0.5%. The system supports a constant loading rate as specified in ASTM D-2166 and is powered by Bluehill Universal software. The system also features a data acquisition rate of up to 5 kHz and various safety and ergonomic enhancements, ensuring reliability and user-friendliness. UCS tests were conducted at a constant strain rate of one percent per minute as specified in the ASTM D-2166 standard.

Figure 3.8 Instron testing device for UCS Testing

3.2.2 UCS Testing Matrix

Clay soil was mixed with two different percentages of polypropylene fiber (0.5% and 1%) and compacted to its maximum dry density. Two samples were tested for each soil-fiber combination and the average strength reported.

Table 3.4 UCS Testing Matrix

Case	ID	Condition
1	BL0	Unreinforced
2	BL0 FR0.5	0.5% Fiber Reinforced
3	BL0 FR01	1% Fiber Reinforced

3.2.3 UCS Sample Preparation

UCS samples had a 4 in. diameter and 8 in. height (**Figure 3.13**). Clay soil was oven dried and sieved through sieve No. 4. Dried soil was mixed at OMC and prepared in five layers using mold and plugs (**Figure 3.9** and **Figure 3.10**). Static loading was applied on the soil sample in the mold to obtain the maximum density (**Figure 3.11** and **Figure 3.12**).

Figure 3.9 Mold and plugs used for UCS sample preparation

Figure 3.10 Soil for UCS sample preparation

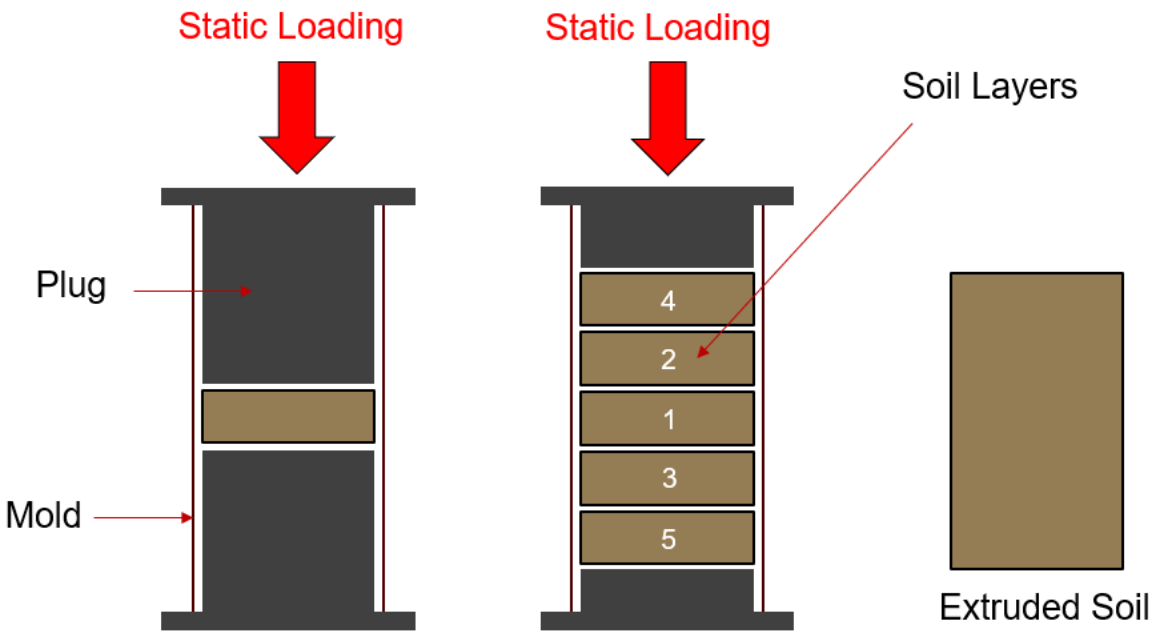

Figure 3.11 Soil sample preparation

Figure 3.12 Static loading setup for UCS sample preparation

Figure 3.13 UCS Sample

3.3 Large-Scale Tracking Wheel (LSTW) Test

3.3.1 Large-Scale Tracking Wheel (LSTW) Apparatus Set-up

The research team at the University of Nebraska-Lincoln designed and constructed the Large-Scale Tracking Wheel (LSTW) testing apparatus. The mechanical performance of fiber-reinforced subgrade was evaluated using the LSTW. The test conditions closely mirror real-world field conditions, particularly in aspects of dimensions and the frequency of rolling wheel loadings. To assess the long-term rutting performance of the subgrade, the team performed rolling wheel loading tests on the clay layer, monitoring the progression of rutting over time. Additionally, the impact of fiber on the strength of pavement layers, as well as the changes in pressure across the clay layer for unreinforced and fiber reinforced soil were evaluated.

The design of the box was taken in part from research performed by Bagshaw et al. (2015) and the Kim et al. (2018) in conjunction with the Georgia Department of Transportation. The test

was conducted for soil-fiber subgrade. The box was one steel piece with additional ribs on the sides to help provide reactionary stiffness. The interior of the box was spray-painted with a black gloss to minimize friction and to prevent rust. The large-scale box was constructed with 5.5-foot wide, 5.5-ft long, and 2.0-ft tall (1.67 meter × 1.67 meter × 0.61 meter) internal dimensions. The layout and the entire assembly are shown in the **Appendix**. The box was placed atop a track that was doweled into the floor. The track was made from c-channel steel with four outer plate extensions with holes in them for the dowels to pass through. These extensions were bolted to the inner track at one end and doweled into place on the other stabilizing the track. The box was attached to a pulley frame which was in turn connected to a motor and the crank arm to push and pull the box in a unidirectional motion. Ten wheels were attached to the bottom of the box to aid with unidirectional movement. The tire used during testing to apply rolling wheel loading on the clay layer surface had a 30-inch diameter with a 7.5-inch width to hold a maximum load of 3000 lbs (1360 kg) (**Figure 3.14**). A mounted ball bearing with two-bolt flange was placed in the wheel and connected to the setup frame by a 6-ft high strength carbon steel rod. This enabled the tire to rotate freely in place.

A hydraulic actuator was used to apply a load of approximately 10 kN through the rectangular steel frame onto the wheel road. The load select criteria was based on works by Kim et al. (2019) where finite element analysis was performed on a 200-meter asphalt concrete layer placed on top of 300-millimeter base layer. The stress distribution across the layer was determined by applying a 40 kilonewton load which is half the load from each tire of a standard single axle (80 kilonewton) load on the surface of the finite element model. It was determined that approximately 75% of the load was reduced in the AC layer with 10 kilonewton distributed to the top of the base layer. The test was run at an approximate speed of 0.447 m/s which is similar to

works by Bagshaw et al. (2015) and Wright et al. (2020) as a way to standardize the testing procedure. The complete set-up is shown in **Figure 3.15**.

Figure 3.14 Tire used for LSTW test

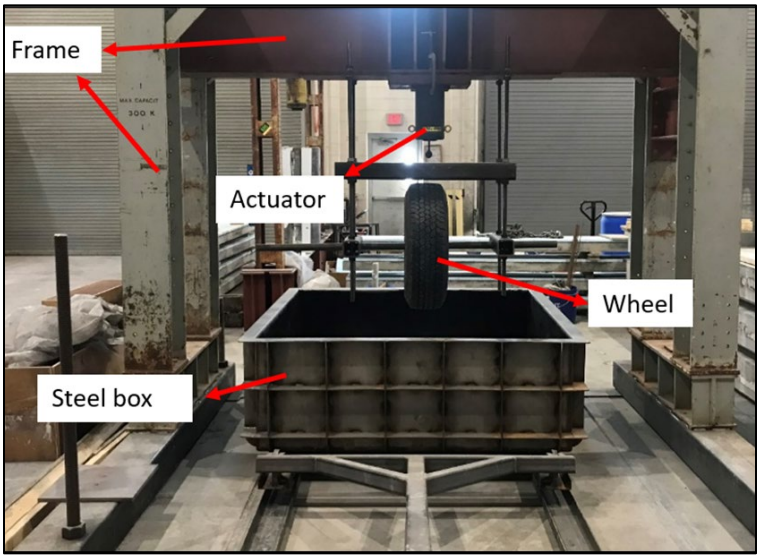

Figure 3.15 Complete set-up of the Large-Scale Tracking Wheel (LSTW) test

3.3.2 Testing Matrix

For the Large-Scale Tracking Wheel test, two distinct scenarios were examined to determine the extent of permanent deformation the clay layer sustains, pressure distribution across the clay layer, and the change in strength/stiffness of the pavement layers due to the use of fiber. Details of these evaluations are presented in **Table 3.5**.

Table 3.5 Large Scale Tracking Wheel (LSTW) testing matrix.

Case	ID	Condition	Layer thickness (in)
1	Control	Unreinforced	8
2	FBR	Fiber Reinforced	8

3.3.2.1 Case 1 – Control Test Preparation

The steel box was filled with 12 in. of sand soil to reduce the boundary condition effect at the base of the steel box. The sand was compacted using a heavy-duty plate compactor as shown in **Figure 3.18** to a relative density of approximately 80%. The compaction of sand layer was performed in two lifts, each approximately six inches.

The clay subgrade soil obtained from the field was air-dried before use (**Figure 3.16**). The lumps of clay were sieved through sieve No. 4. The portion retained on sieve No. 4 (4.75mm) was then ground using a soil grinder (**Figure 3.17**). The clay soil that passed sieve No. 4 (4.75mm) was mixed at OMC (18%) using a concrete mixer and was placed in the steel box (**Figure 3.19**). The clay soil at OMC was compacted with a heavy-duty plate compactor (**Figure 3.18**) to a relative density approximately 90% (**Figure 3.20**). The compaction of the clay layer was performed in two lifts approximately 4 in. thick each. The total height of the clay layer was 8 in.

Figure 3.16 Air drying of clay soil

Figure 3.17 Grinding of clay soil lumps.

Figure 3.18 Heavy duty plate compactor.

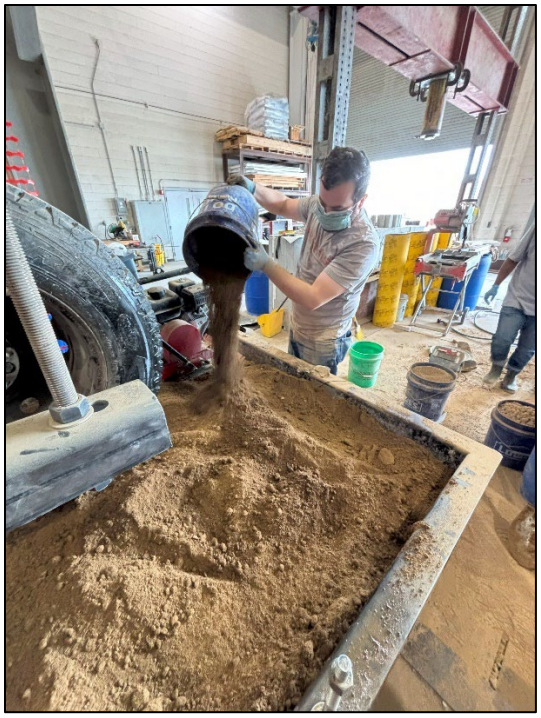

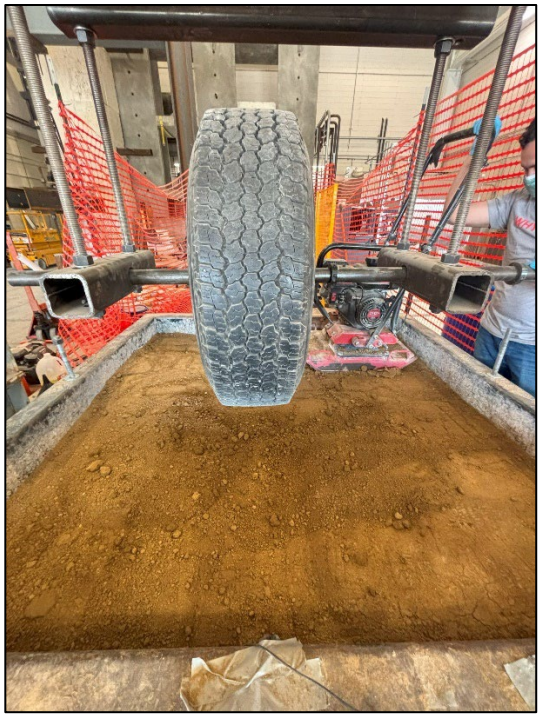

Figure 3.19 Placement of clay soil in steel box **Figure 3.20** Compacted clay soil layer.

3.3.2.2 Case 2 – Fiber Reinforced Test Preparation

For this case, polypropylene fiber was incorporated into the clay soil at a selected percentage of 1%, which was determined based on the results from UCS testing with various soil-fiber combinations. To ensure an even distribution of the fibers within the soil, careful attention was given to the mixing process. The clay-fiber mix was prepared at OMC using a concrete mixer. To avoid clumping and achieve a uniform blend, the fibers were gradually introduced into the soil while the mixer was running, allowing for thorough integration throughout the mixture. Once the mixing process was complete, the fiber-soil mixture was placed on the sand layer and compacted in a manner consistent with the control case. The mixture was compacted in two lifts, each approximately four inches thick, resulting in a total height of eight inches. This methodical

approach ensured that the fibers were evenly distributed throughout the compacted layers, leading to consistent and reliable test results (see **Figure 3.21**).

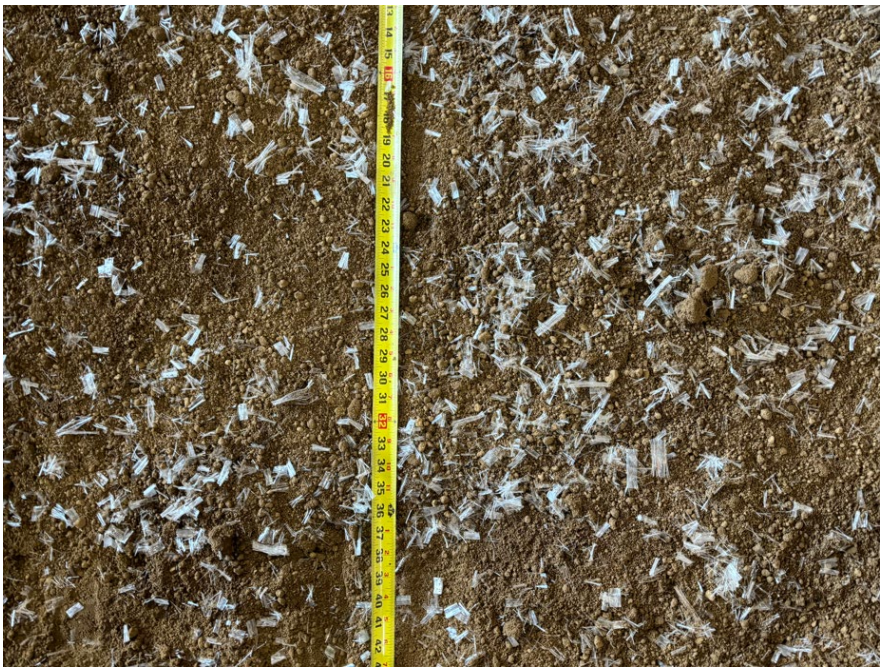

Figure 3.21 Compacted clay-fiber layer.

3.3.3 Large Scale Tracking Wheel Test Instrumentation

3.3.3.1 Linear Variable Displacement Transducer

Four LVDTs from Harold G. Schaevits Industries with a measuring range of 2 in. were used to record the vertical deformation of the base layer. These were made from industrial duty material for resistance to dust, temperature, shock and variable. The vertical deformation recorded showed how rutting progressed during the test. These were fixed along a wooden beam that was held in place by a threaded rod on the sides of the steel box with bolts at the top and bottom to prevent movement during testing. The LVDTs were installed along the center of the steel box on a wooden beam as shown in **Figure 3.22**. All LVDTs were calibrated before usage. The coefficient

of determination (R^2) for LVDTs, representing the relationship between the voltage and calibrated readings, ranges from 0.9979 to 0.9996, as highlighted in **Table 3.6**. This range signifies the accuracy and precision of the LVDTs readings. The LVDTs were connected to a Keysight DAQ970A 20-channel data logger using the Benchvue software.

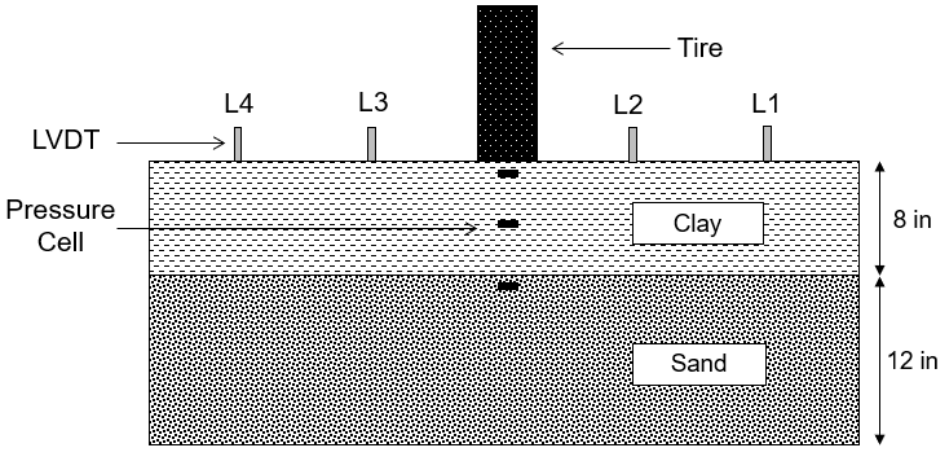

Figure 3.22 LVDT positions in steel box

Table 3.6 LVDT R^2 summary

LDVT	**R^2**
1	0.9996
2	0.9996
3	0.9979
4	0.9982

3.3.3.2 Spring Potentiometer

The UniMeasure LX-PA-20 Series linear position transducer is a low cost, compact transducer with a measuring range of 500 mm. This transducer was connected to the frame and wheel shaft to measure the deformation that occurred at the clay layer. The string potentiometer was calibrated before use. The R^2 for the transducer was obtained as 0.99.

3.3.3.3 Pressure Cells

Three stainless steel pressure cells with excellent corrosion resistance from Tokyo Measure Instrument Lab were used for the test. They have a 50 mm outer diameter and a dual diaphragm structure (**Figure 3.23**). The pressure cells were calibrated by applying different loads with the help of a calibrated actuator. A linear trend was established from which an equation was obtained for the relationship between the pressure and output voltage. The R^2 for the three pressure cells used are found in **Table 3.7**. The pressure sensors were also connected to a Keysight DAQ970A 20-channel data logger using the Benchvue software.

One pressure cell was installed on the compacted sand layer which is also the interface of the sand and clay layer (**Figure 3.24**). A second pressure cell was installed mid-height in the clay layer approximately 4 in. from the surface with a third pressure cell installed on top of the clay layer (**Figure 3.25**). These pressure cells were used to monitor pressure distribution across the layers during testing. The schematic of the individual pressure cell positions can be seen in **Figure 3.26**.

Table 3.7 Pressure Cell R^2 Summary.

Pressure Cell	**R^2**
1	0.9999
2	0.9996
3	0.9990

Figure 3.23 TML Pressure cells.

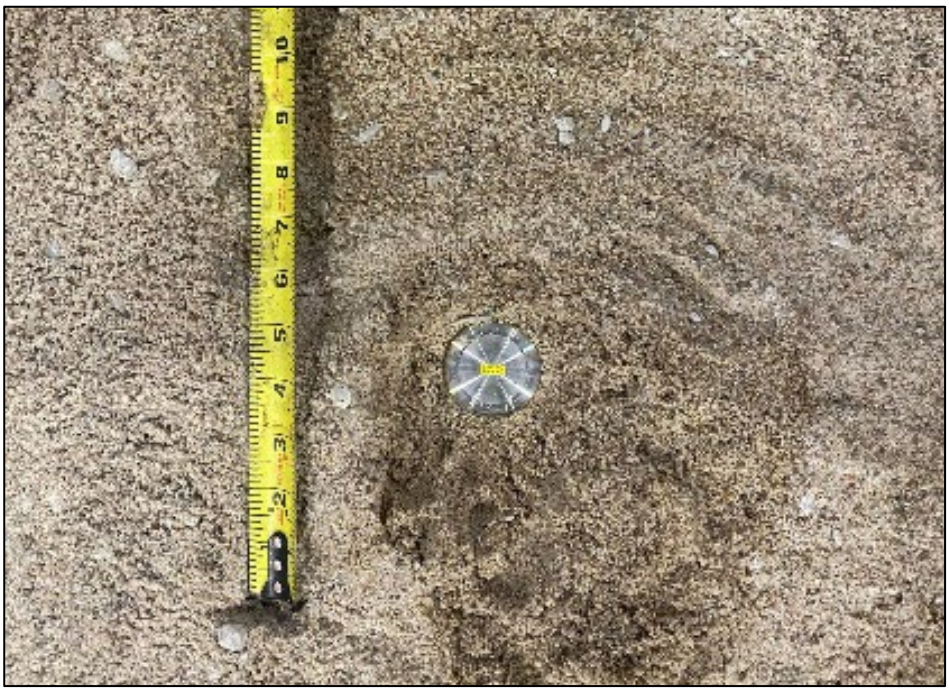

Figure 3.24 Pressure cell on compacted sand layer.

Figure 3.25 Pressure cell on compacted clay layer.

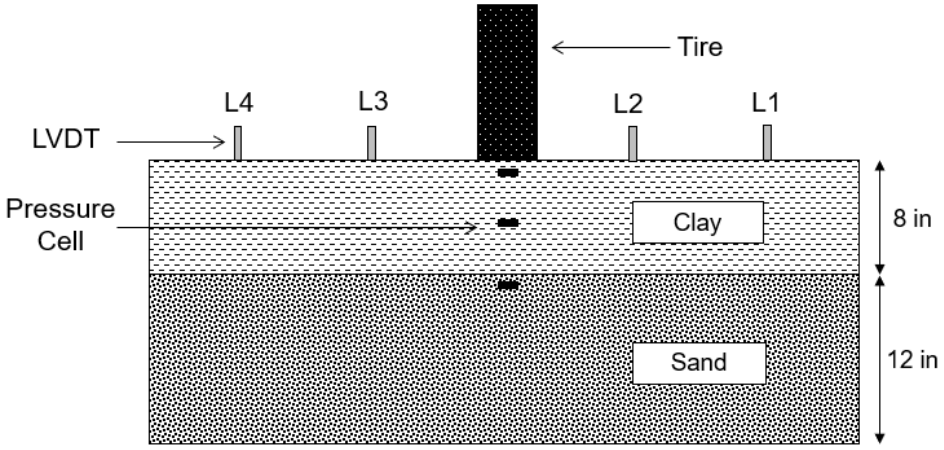

Figure 3.26 Schematic of pressure cell positions (unit, inches).

3.3.3.4 Load Cell

A load cell was installed beneath the hydraulic piston to measure the load that would be applied during the test as shown in **Figure 3.27** and **Figure 3.28**. Assisted by an electric hydraulic pump system, an approximate load of 10 kN was applied through the actuator for reasons mentioned in 3.3.1. The applied load was continuously monitored using a load cell and adjusted throughout testing.

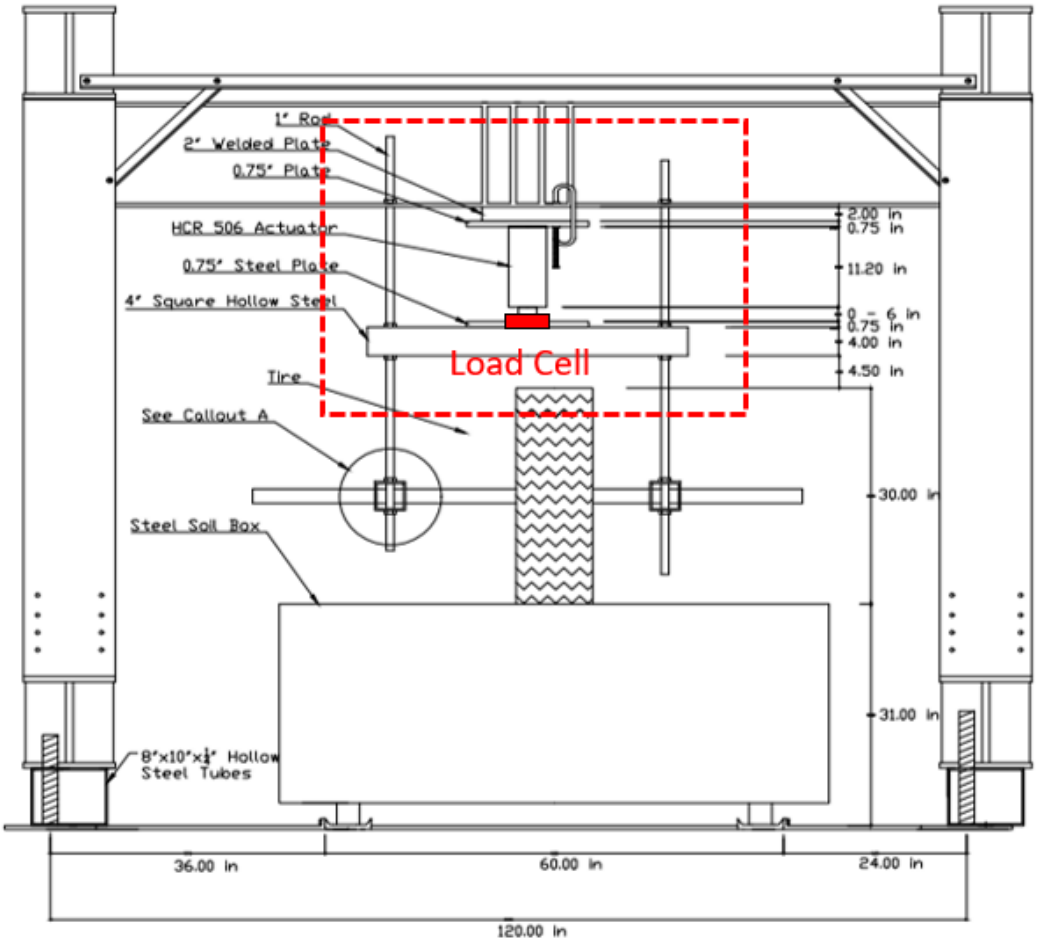

Figure 3.27 Schematic of load cell position (unit, inches).

Figure 3.28 Load cell positioned beneath actuator.

3.3.4 Test Run

The load cell, linear vertical displacement transducers (LVDTs), string potentiometer and pressure cells were connected to their respective power supply units and the data acquisition system. The data acquisition box was connected to a laptop to record the data during testing. The wheel was gently lowered onto the surface of the steel box. A 10 kN load was applied on the surface of the layers. The test setup was then turned on from the control unit initiating the unidirectional motion of the box at a speed of approximately 1 mph. The complete testing setup is shown in **Figure 3.29**. Results for each case are discussed further in **Section 4.2.**

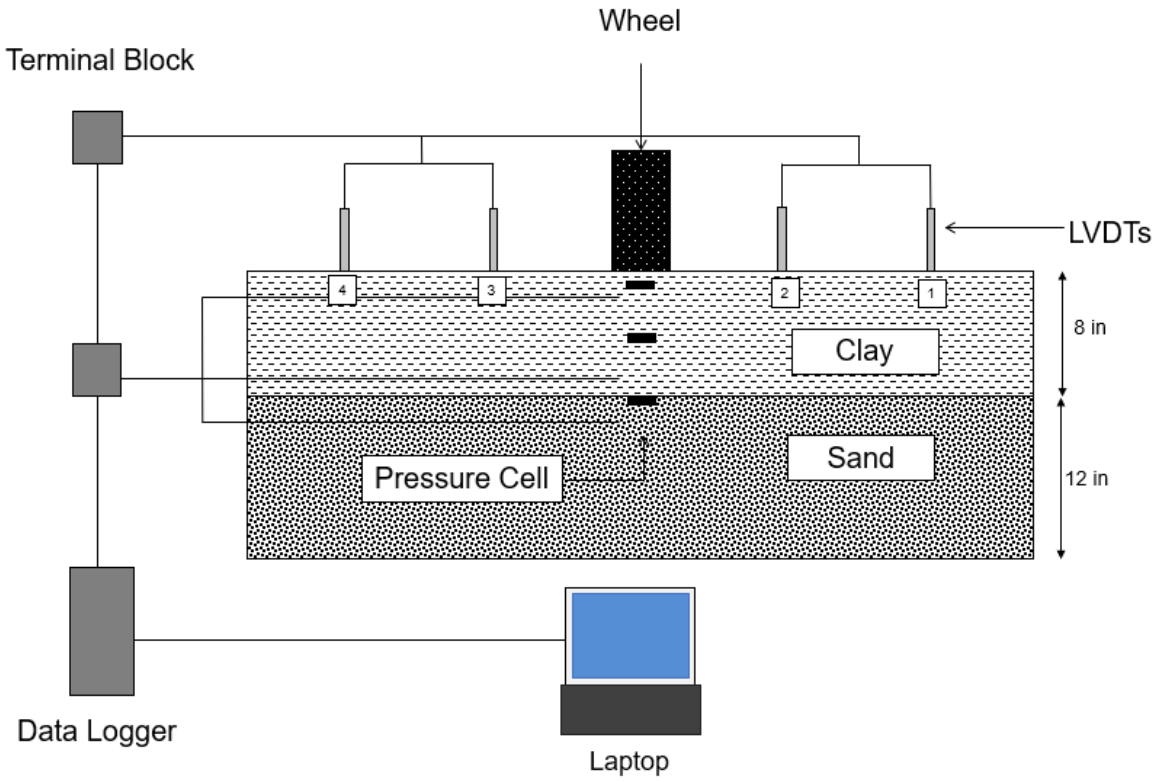

Figure 3.29 LSTW complete test setup.

3.3.5 Dynamic Cone Penetrometer (DCP) Test

The Dynamic Cone Penetration Test provides a measure of a material's in-situ resistance to penetration. The schematic of the DCP device is shown in **Figure 3.30**. The number of blows required for the cone to penetrate a specific depth (usually measured in mm/blow) gives an indication of the soil's strength and is called the Dynamic Penetration Index (DPI). This test was conducted before and after applying rolling wheel loads to the surface of the prepared pavement layers (**Figure 3.31**). The DPI was correlated with resilient modulus to provide an indication of how the stiffness/strength within the pavement layer changes for both geosynthetic reinforced and unreinforced cases.

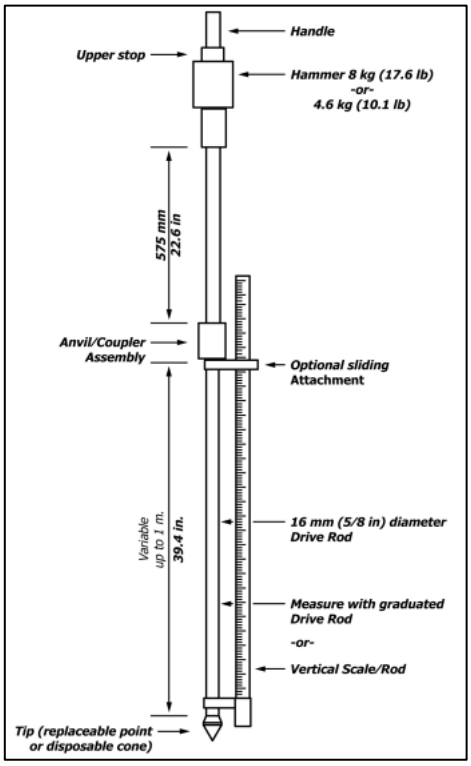

Figure 3.30 Schematic of DCP device

Figure 3.31 DCP test on compacted clay layer

Chapter 4 Results and Discussion

4.1 Analysis of UCS test results

The control case (unreinforced) showed a peak UCS value of 70 psi followed by a rapid decline in peak strength. The soil-fiber mixture with 0.5% of polypropylene fiber had a UCS strength value of approximately 65 psi while the UCS of the soil-fiber mixture with 1% fiber showed a higher strength in UCS with a peak value of approximately 74 psi. The strain hardening effect was seen in the two soil-fiber combination cases, implying a greater residual strength. **Figure 4.1** shows the stress strain curves for clay soil-fiber mixtures. The summary of the peak strength for three cases are shown in **Table 4.1**. This strain hardening effect is due to the interaction of soil with fiber through adhesion and friction (Madrid et al. 2024). For the control case, the sharp strength reduction can be attributed to the weak inter-particle bonds of the soil material (Skempton 1970). These interparticle bonds may contribute as a glue to connect the particles to each other. The quality of the inter-particle bonds may be dependent on the clay mineralogy (Li et al. 2013). Based on the UCS results, the mixture with 1% polypropylene fiber combination was selected for the large-scale tracking wheel test. This combination provided the best performance in terms of peak and residual strength of the clay-soil mixtures.

Table 4.1 Peak and residual strength for different cases

Case	Peak strength (psi)	Residual strength (psi)	Percentage reduction (%)
BL0	70	20	71.4
BL0FR0.5	65	31	52.3
BL0FR1	74	48	35.1

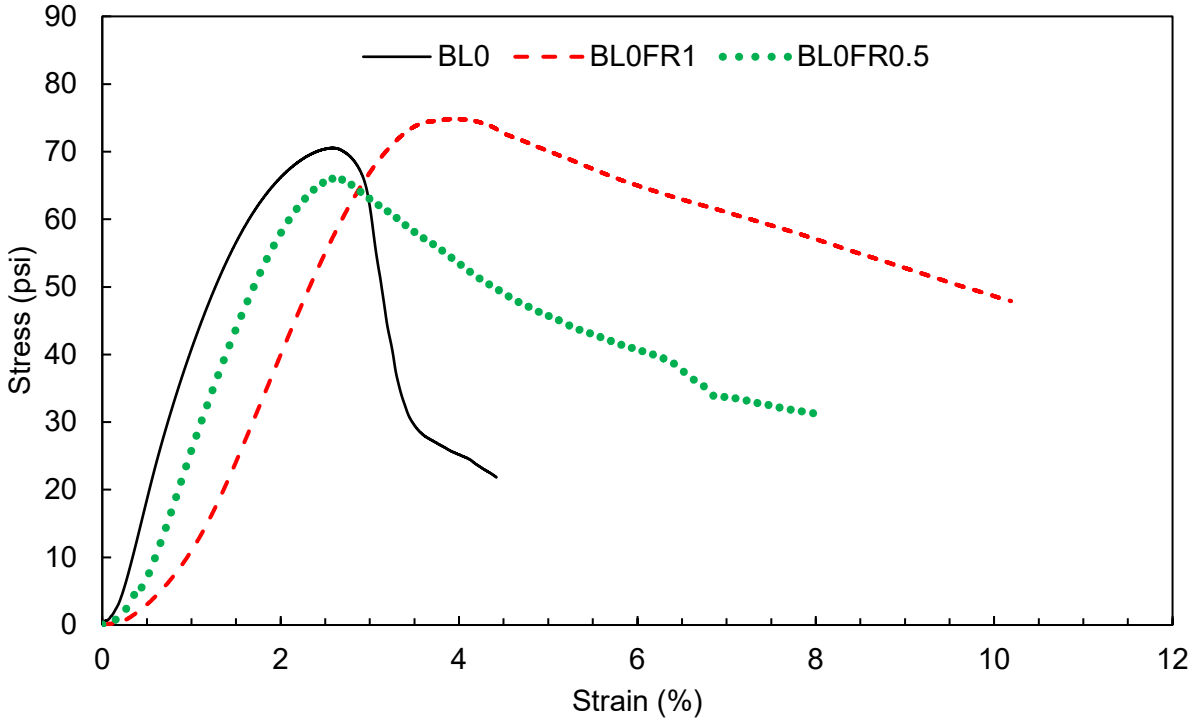

Figure 4.1 Stress-strain curve for clay soil with fiber

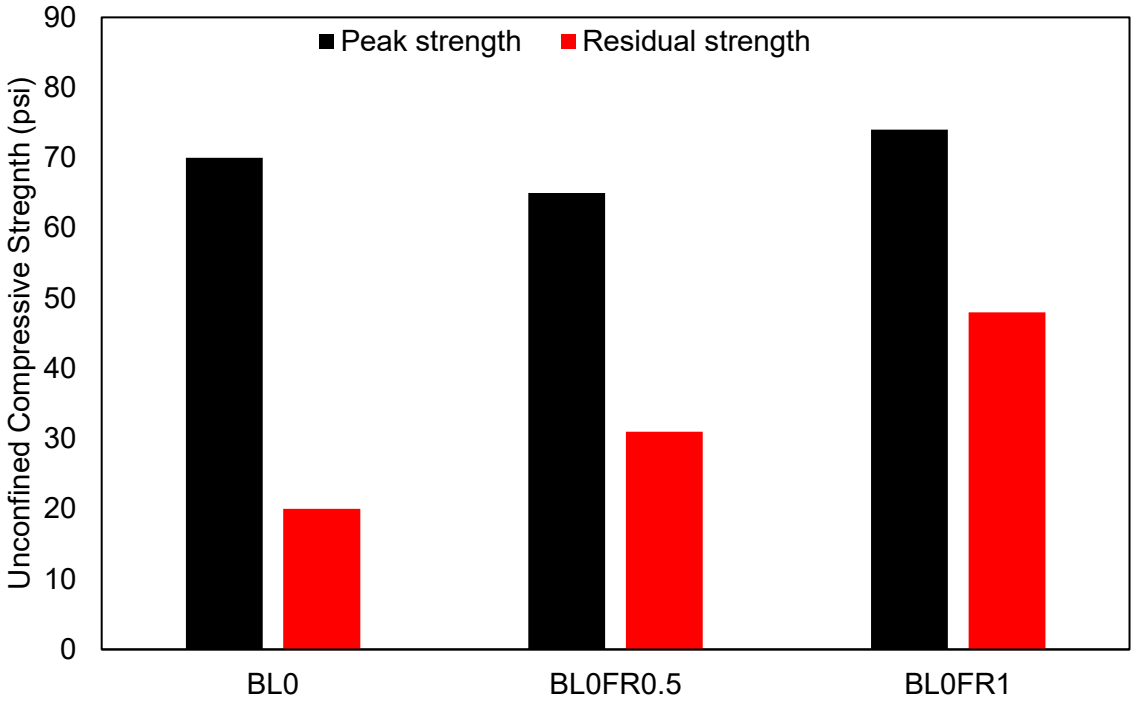

Figure 4.2 UCS of soil-fiber mixtures

4.2 Analysis of LSTW test results

Three key parameters were assessed across the three cases to understand the impact of the use of fiber with clay soil. This included strength/stiffness, as reflected by Dynamic Cone Penetration (DCP) indices (DPI), permanent deformation, and the pressure changes.

4.2.1 Evaluation of Pavement Strength/Stiffness

DCP tests were conducted before and after applying the rolling wheel test on the pavement layer of the LSTW test to evaluate the change in strength of the pavement layer. **Figure 4.3** shows the cumulative blows against depth for the two cases. The DPI obtained from the DCP test along the clay and sand layers can be found in **Figure 4.4**. The fiber reinforced case showed a better performance in terms of layer strength/stiffness both before and after the rolling wheel load application. The summary of the average DCP for both unreinforced and fiber reinforced cases can be found in **Table 4.2**. **Figure 4.5** shows the reduction in the layer DPI for the fiber reinforced case compared to the unreinforced case.

Table 4.2 Summary of DPI for unreinforced and fiber reinforced cases

Layer		Clay	
Case		Control	Fiber reinforced
DPI (mm/blow)	Before	59.7	51.3
	After	27	21.6

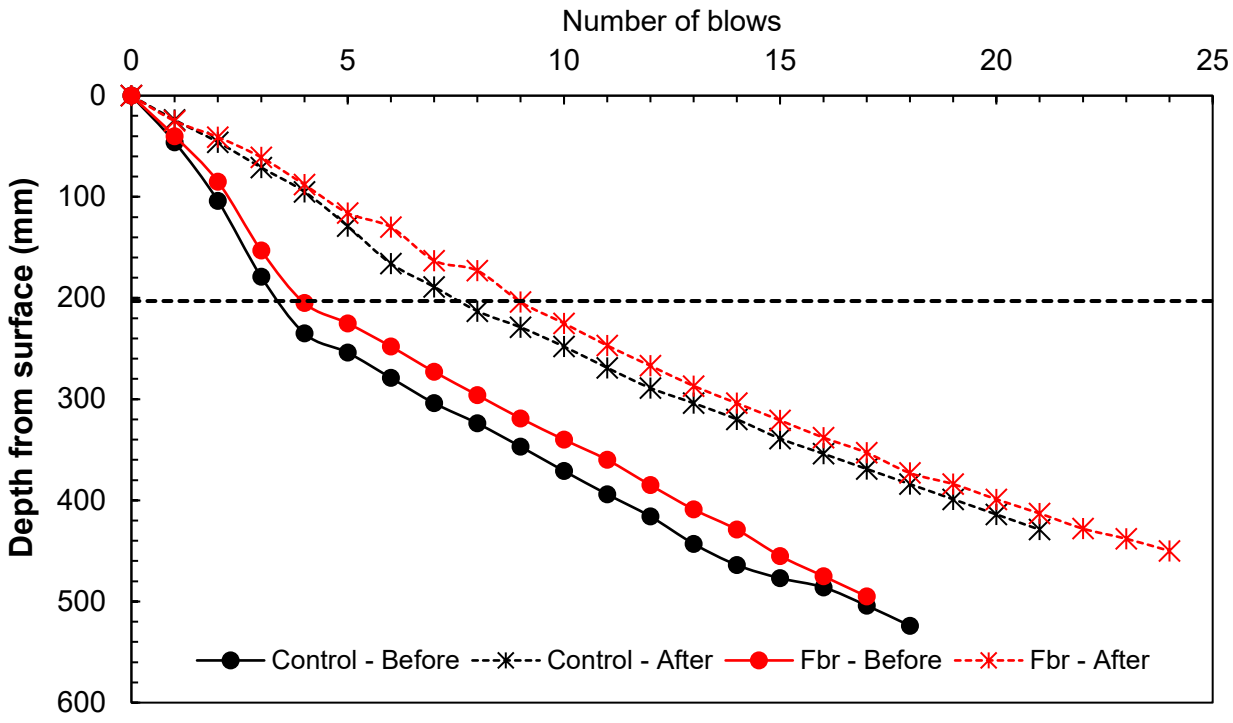

Figure 4.3 Cumulative blows vs depth for unreinforced and fiber reinforced cases

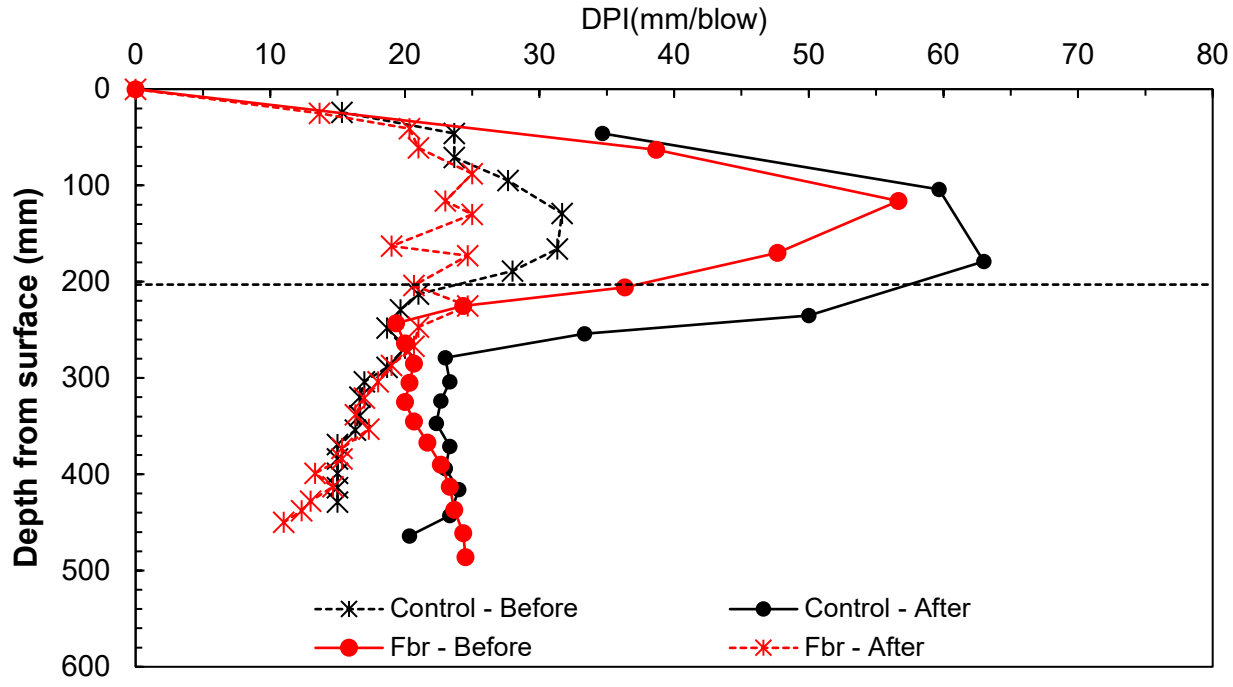

Figure 4.4 DPI vs Depth for unreinforced and fiber reinforced cases

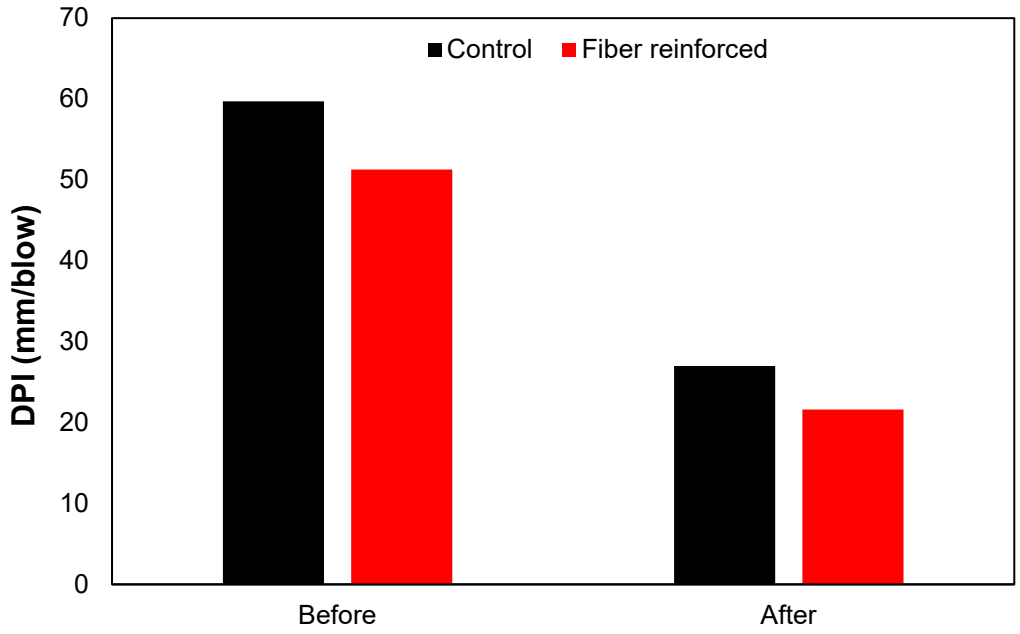

Figure 4.5 DPI comparison for unreinforced and fiber reinforced cases before and after rolling wheel loading

4.2.2 Correlation between DPI and other parameters

Using correlations by Herath et al. (2005) and the U.S. Army Corps of Engineers the Mr (Eq. 1) and CBR (Eq. 2) of the clay soil were computed from the DPI for the two cases evaluated as shown in **Table 4.3**. **Figure 4.6** shows a higher resilient modulus of 8% for the fiber reinforced than for the control case before the rolling wheel load was applied. This increase in resilient modulus for the fiber reinforced case can be attributed to the interaction between the soil and fiber creating a stronger bond. After the rolling wheel load application, the resilient modulus of the fiber reinforced soil as compared to the control case increased by 17%. This increase can be attributed to densification of the clay layer from the rolling wheel load application and the higher residual strength of the fiber reinforced case as compared to the control.

$$Mr = 16.28 + 928.24/DPI \quad (1)$$

$$CBR = 292/(DPI)^{1.12} \quad (2)$$

Table 4.3 Correlation of Mr and CBR derived from DPI before (B) and after (A) exposure to wheel rolling load.

Case	Correlation	DPI (mm/blow)		Mr (MPa)		CBR (%)	
				Herath et al (2005)		(US Army Corps)*	
		B	A	B	A	B	A
Control	Clay	59.7	27	31.8	50.7	3.0	7.3
Fiber reinforced	Clay	51.3	21.6	34.4	59.3	3.5	9.3

Table 4.4 Change in Mr for unreinforced and fiber-reinforced cases before (B) and after (A) exposure to wheel rolling load.

Case	Mr (MPa)		Percentage change (%)
	Herath et al (2005)		
	B	A	
Control	31.8	50.7	59.2%
Fiber reinforced	34.4	59.3	72.4%
Percentage change (%)	8.0%	17.0%	

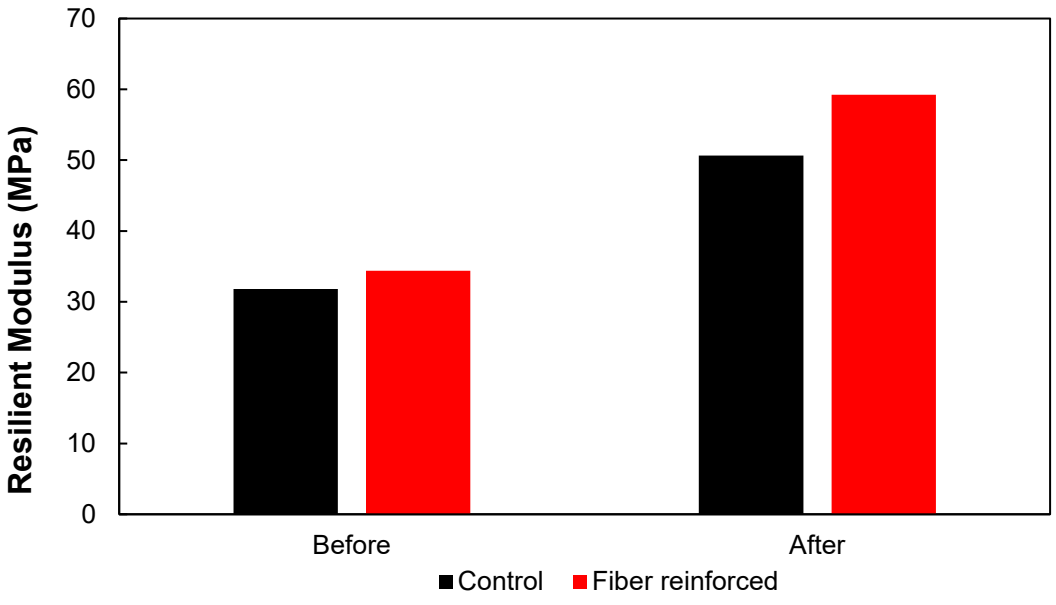

Figure 4.6 Estimated resilient modulus from correlation – Clay.

4.2.3 Evaluation of Permanent Deformation (Rutting)

The total vertical deformation that occurred at the top surface of the clay course layer was obtained after the rolling wheel load was applied for the two cases using the string potentiometer. The deformation was recorded directly using a measuring tape for confirmation. **Figure 4.9** shows the total deformation recorded for both unreinforced and fiber reinforced cases. The test was terminated after total deformation stabilized. The reduction in total deformation by 14.7% was observed for the fiber reinforced cases compared to the control case.

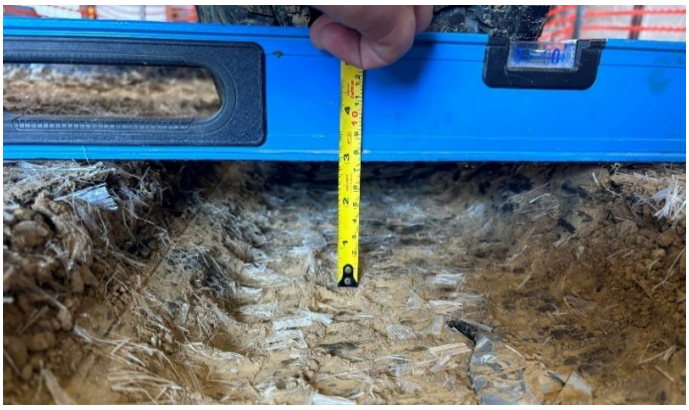

Figure 4.7 Deformation measurement with measuring tape for fiber reinforced case

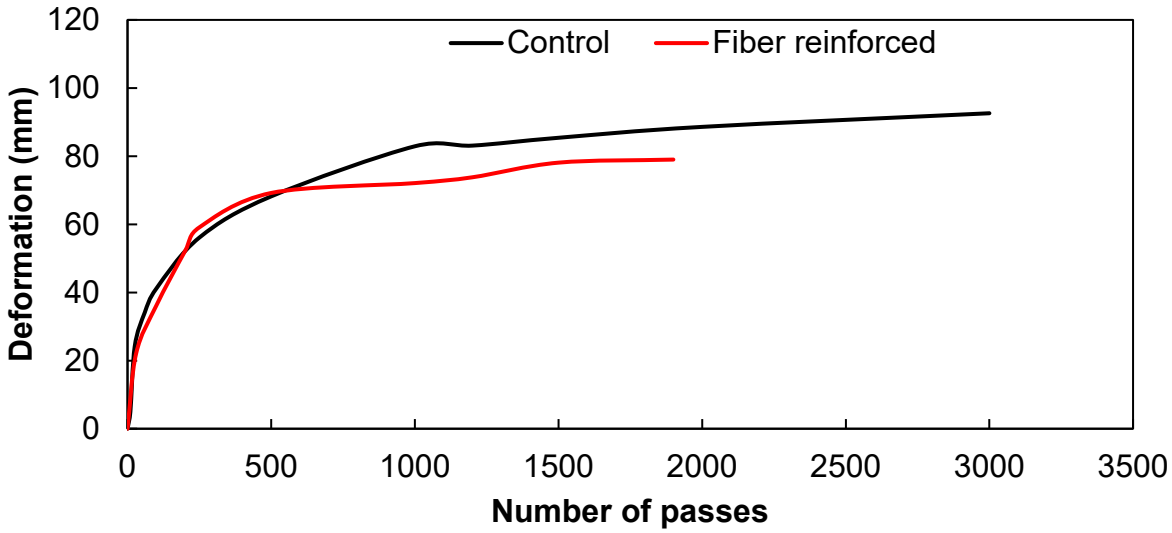

Figure 4.8 Deformation recorded from spring potentiometer

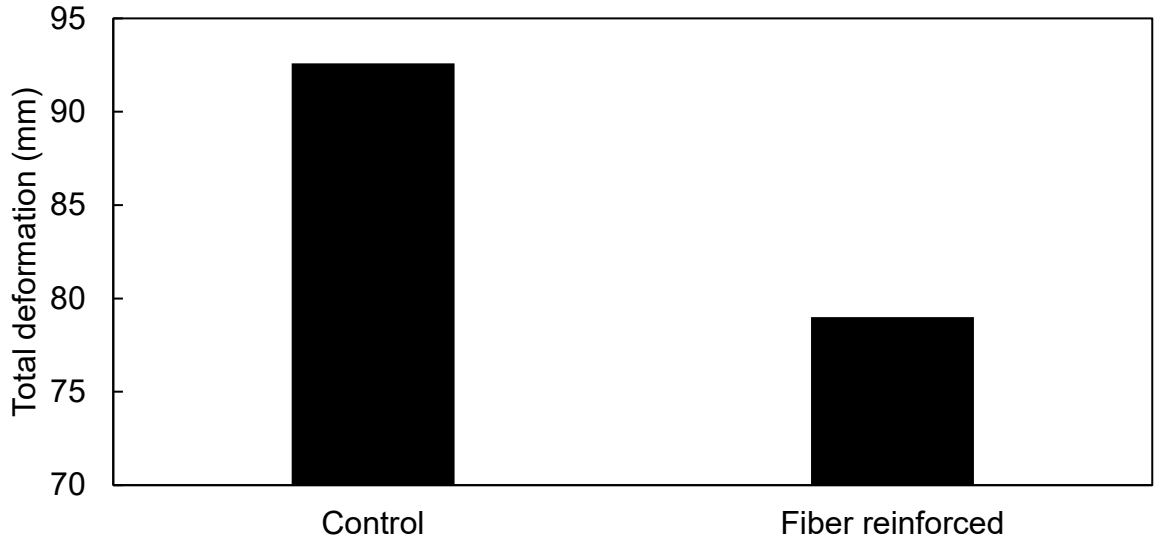

Figure 4.9 Total deformation for fiber reinforced and unreinforced cases

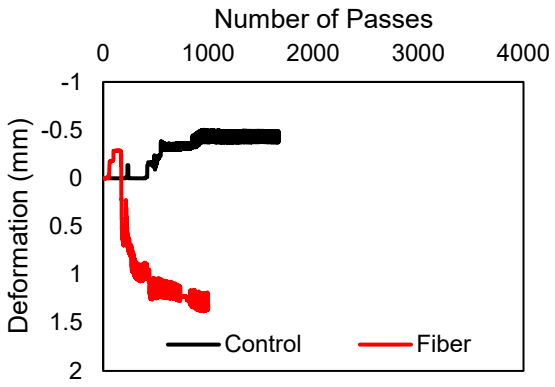

Figure 4.10 LVDT 2 deformation readings.

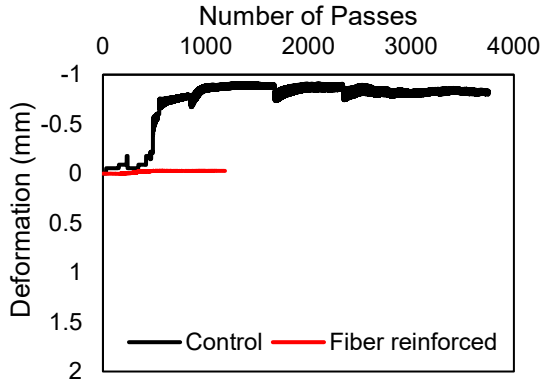

Figure 4.11 LVDT 3 deformation readings.

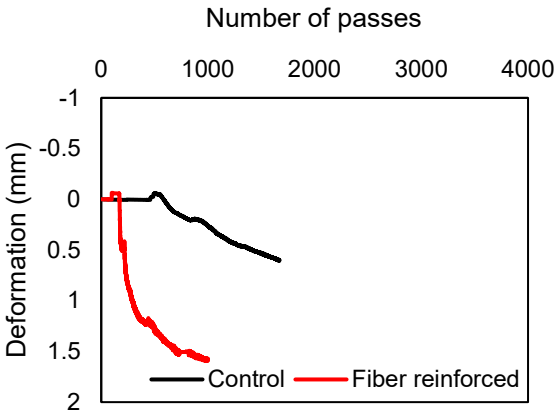

Figure 4.12 LVDT 1 deformation readings

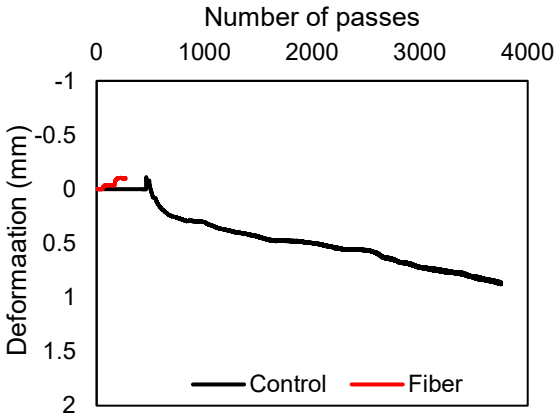

Figure 4.13 LVDT 4 deformation readings.

4.2.4 Pressure Reduction Effect

Figure 4.15, **Figure 4.16** and **Figure 4.17** show pressure distribution profiles for the top, middle, and bottom pressure cells taken over a 30 second period. The peaks in the pressure cells reading shows the point at which the wheel is directly above the pressure cells. **Table 4.5** and **Figure 4.18** show a summary of the pressure cell readings for the top, middle, and bottom pressure cells. The pressure values represent the stress experienced at different depths within the soil layer under the applied load. Specifically, the top pressure cell records the stress closest to the wheel, the middle pressure cell measures stress at mid-depth, and the bottom pressure cell captures the

stress near the base of the soil layer. For the top pressure cell, the average maximum reading obtained in both the control and fiber reinforced cases are approximately equal. The bottom pressure cell for the fiber reinforced case had a lower peak pressure cell reading of 67.5 kPa compared to the control case with an average peak pressure of 71.7 kPa. This represents a 5.8% pressure reduction recording in the bottom pressure cell for the fiber reinforced case. This reduction suggests that the inclusion of fiber enhances the distribution of stress within the soil layer, reducing the stress concentration at the base and thus potentially improving the overall stability of the subgrade. Fiber inclusion can enhance the tensile strength and shear resistance of soils, leading to better load distribution and improved stability (Li and Zornberg 2019; Mirzababaei et al. 2018).

Table 4.5 Average peak pressure for top, middle and bottom pressure cells

Case	Pressure (kPa)		
	Top	Middle	Bottom
Control	152.1	119.4	71.7
Fiber reinforced	151.3	129.0	67.5
Percentage change	0.5%	-8.0%	5.8%

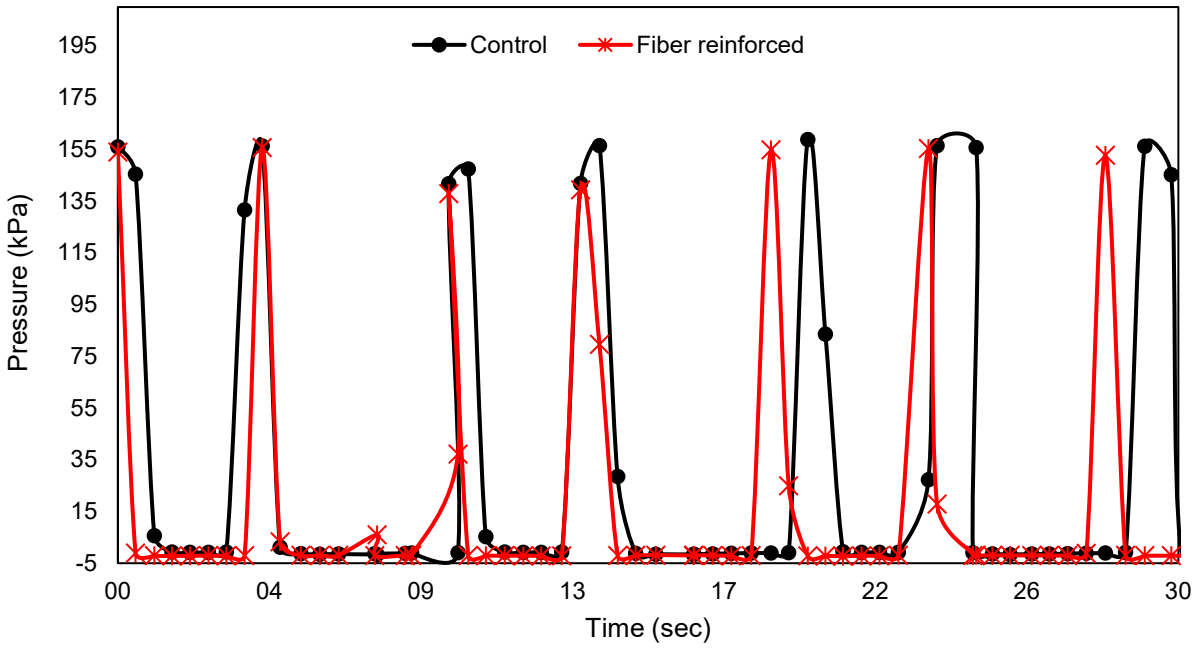

Figure 4.14 Top pressure cell reading over 30-second period

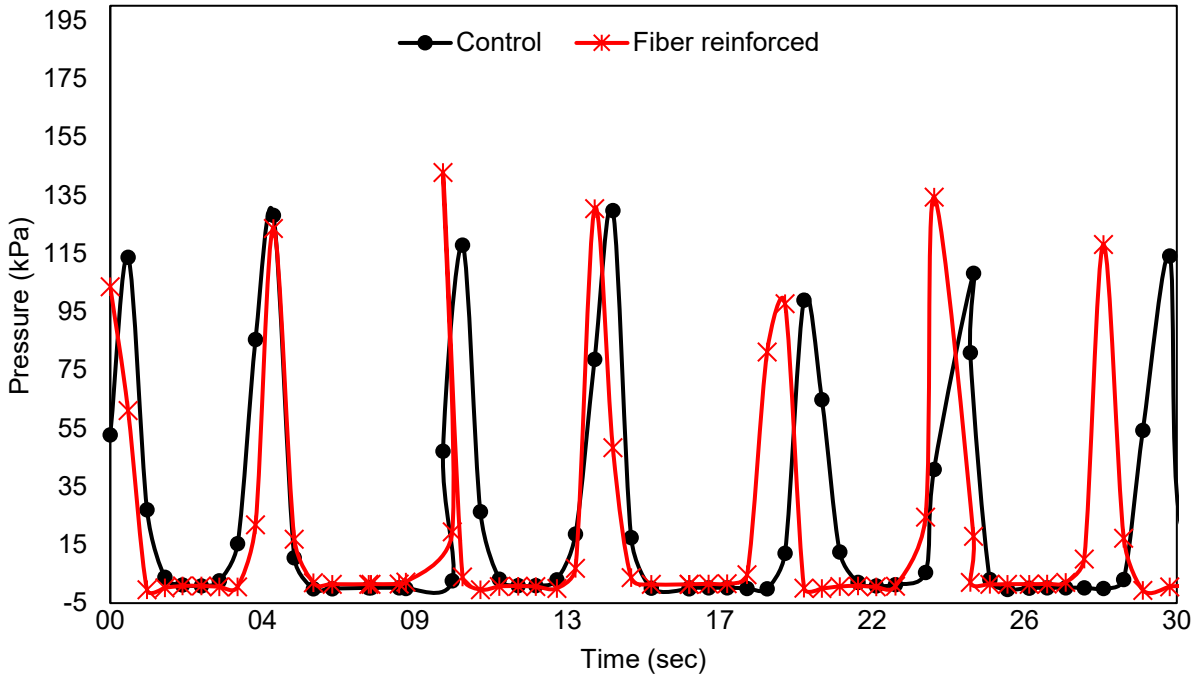

Figure 4.15 Middle pressure cell reading over 30-second period

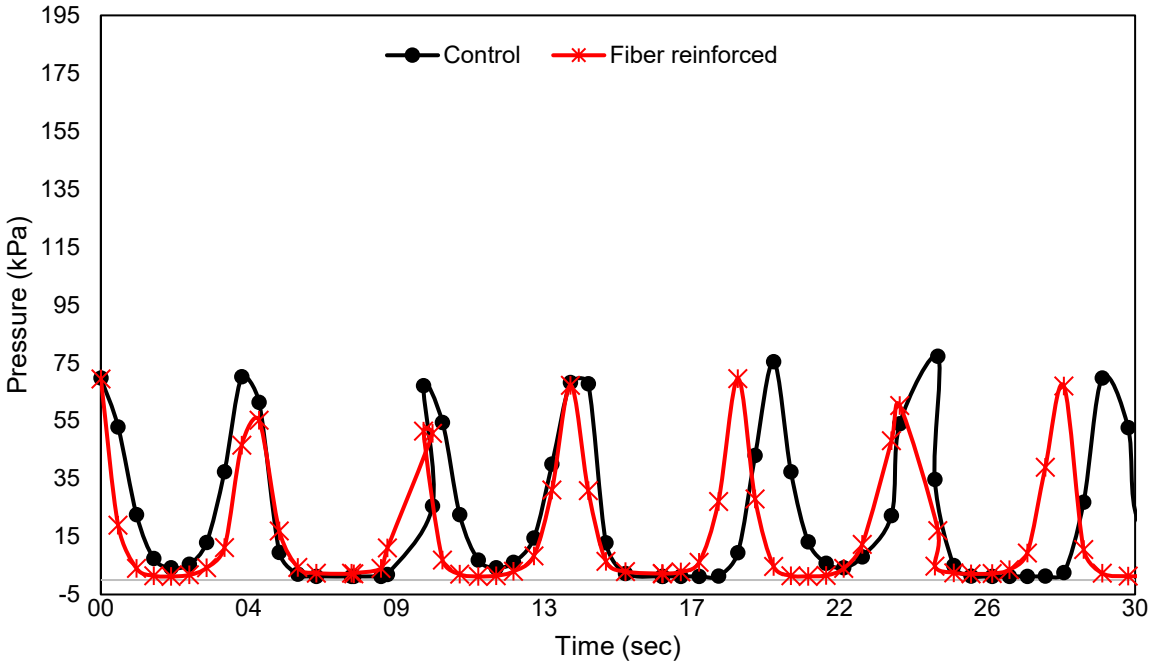

Figure 4.16 Bottom pressure cell reading over 30-second period

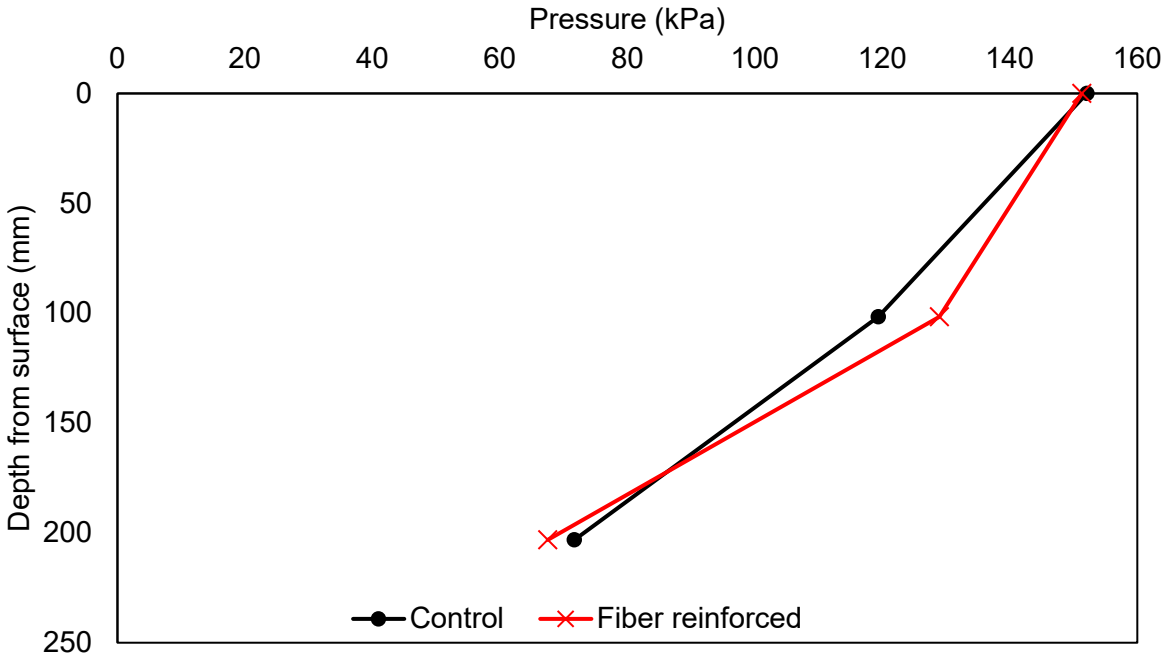

Figure 4.17 Pressure distribution across clay layer

Chapter 5 Conclusions

This study was to evaluate the performance of the polypropylene fiber reinforced subgrade to provide a better understanding of the significant effect fiber has on soil reinforcement. Extensive experimental work through Unconfined Compressive Strength (UCS) testing and Large-Scale Tracking Wheel Testing (LSTW) were performed to evaluate various parameters and the effect of the polypropylene fiber reinforcement on the clay subgrade. The parameters included Peak and Residual strength from UCS testing, the material's strength and stiffness which the Dynamic Cone Penetrometer Index (DPI) indicates was analyzed, and deformation reduction and pressure distribution effects to compare the performance of reinforced and unreinforced sections.

The benefits of the fiber reinforcement application found from this study include a higher UCS of approximately 5.7% as compared to an unreinforced case. The strain hardening effect was observed for polypropylene fiber reinforced cases which results in a residual strength of fiber reinforced soil being approximately 140% times the control case for a fiber content of 1%. From the LSTW test, an 8% increase in resilient modulus of soil-fiber combination was observed before rolling wheel loading was applied.

After rolling wheel loading was applied for the unreinforced and reinforced cases, the difference in resilient modulus increased to 17%. This can be attributed to the increased soil-fiber interaction resulting in a stiffer soil layer. The resilient modulus was obtained using DPI from DCP tests and resilient modulus correlations from Herath et al. (2005). Also, for the fiber reinforced case, a relatively lesser deformation of approximately 14.7% was observed compared to the unreinforced case. The pressure acting on the bottom pressure cell for the fiber reinforced case reduced by 5.8%, implying distribution of the stress within the layer as a result of the fiber. These results highlight the benefit of using fiber as a reinforcing agent for soil subgrade, however, the

application fiber should be a case-by-case study because of the variable site conditions and soil types. More studies are required to evaluate how different fibers perform with different soil types to provide a better understand of the ideal fiber type for a particular soil.

References

Divya, P.V., Viswanadham, B.V.S. and Gourc, J.P., 2014. Evaluation of tensile strength-strain characteristics of fiber-reinforced soil through laboratory tests, Journal of Materials in civil Engineering, 26(1), pp.14-23.

Gao, L., Hu, G., Xu, N., Fu, J., Xiang, C. and Yang, C., 2015. Experimental study on unconfined compressive strength of basalt fiber reinforced clay soil, Advances in Materials Science and Engineering, 2015.

Gregory, G. H. 2006. Shear Strength, Creep and Stability of Fiber-Reinforced Soil Slopes, Ph.D. Dissertation, Oklahoma State University, Stillwater, OK, USA.

Hensley, T.T., Jensen, W.G. and Berryman, C.W., 2007. Pozzolan stabilized subgrades (No. SPR-1 (06) 578).

Li, C. and Zornberg, J.G., 2019. Shear strength behavior of soils reinforced with weak fibers, Journal of Geotechnical and Geoenvironmental Engineering, 145(9), p.06019006.

Li, Y. 2013. Effects of particle shape and size distribution on the shear strength behavior of composite soils. Bulletin of Engineering Geology and the Environment, 72, 371-381.

Mirzababaei, M., Arulrajah, H., Horpibulsuk, S., Soltani, A., Khayat, N., 2018. Stabilization of soft clay using short fibers and poly vinyl alcohol, Geotext. Geomembr. 46, 646–655.

Maher, M.H. Ho, Y.C. 1994. Mechanical properties of kaolinite/fiber soil composite, J. Geotech. Eng. 120 1381–1393, doi:http://dx.doi.org/10.1061/ (asce)0733-9410(1994)120:8(1381).

Skempton, A. W. (1970). First-time slides in over-consolidated lays. *Geotechnique*, *20*(3), 320-324.

Sujatha, E. R., Atchaya, P., Darshan, S., & Subhashini, S. 2021. Mechanical properties of glass fibre reinforced soil and its application as subgrade reinforcement. *Road Materials and Pavement Design*, *22*(10), 2384-2395.

Tang, C.S., Wang, D.Y., Cui, Y.J., Shi, B. and Li, J., 2016. Tensile strength of fiber-reinforced soil. Journal of Materials in Civil Engineering, 28(7), p.04016031.

Zheng, B, Zhang, D, Liu, W., Yang, Y., Yang, H., 2019. Use of basalt fiber-reinforced tailings for improving the stability of tailings dam, Materials (Basel) 12 1306, doi:http://dx.doi.org/10.3390/ma12081306.

Appendix A The Large-Scale Tracking Wheel Test Drawings

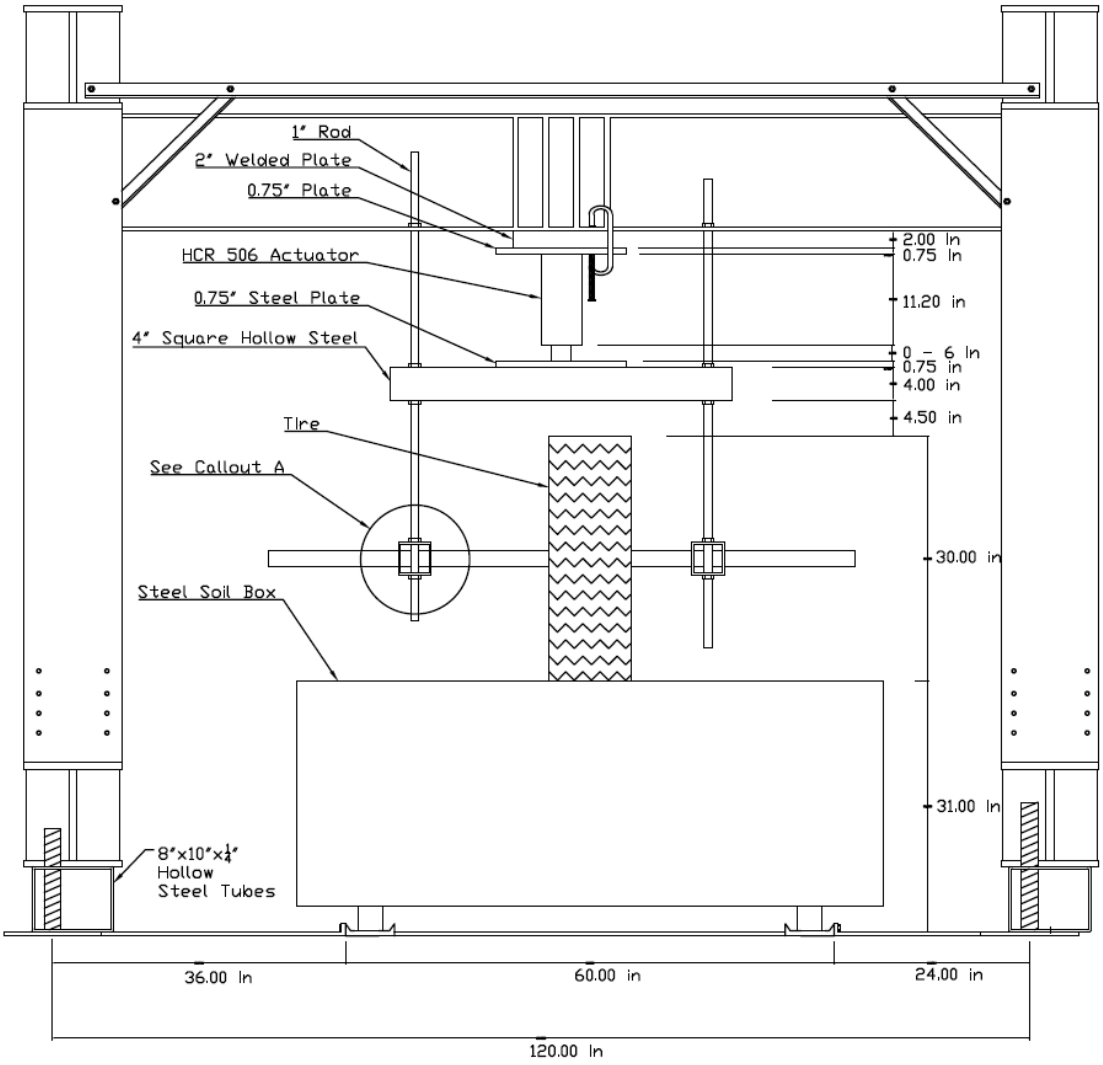

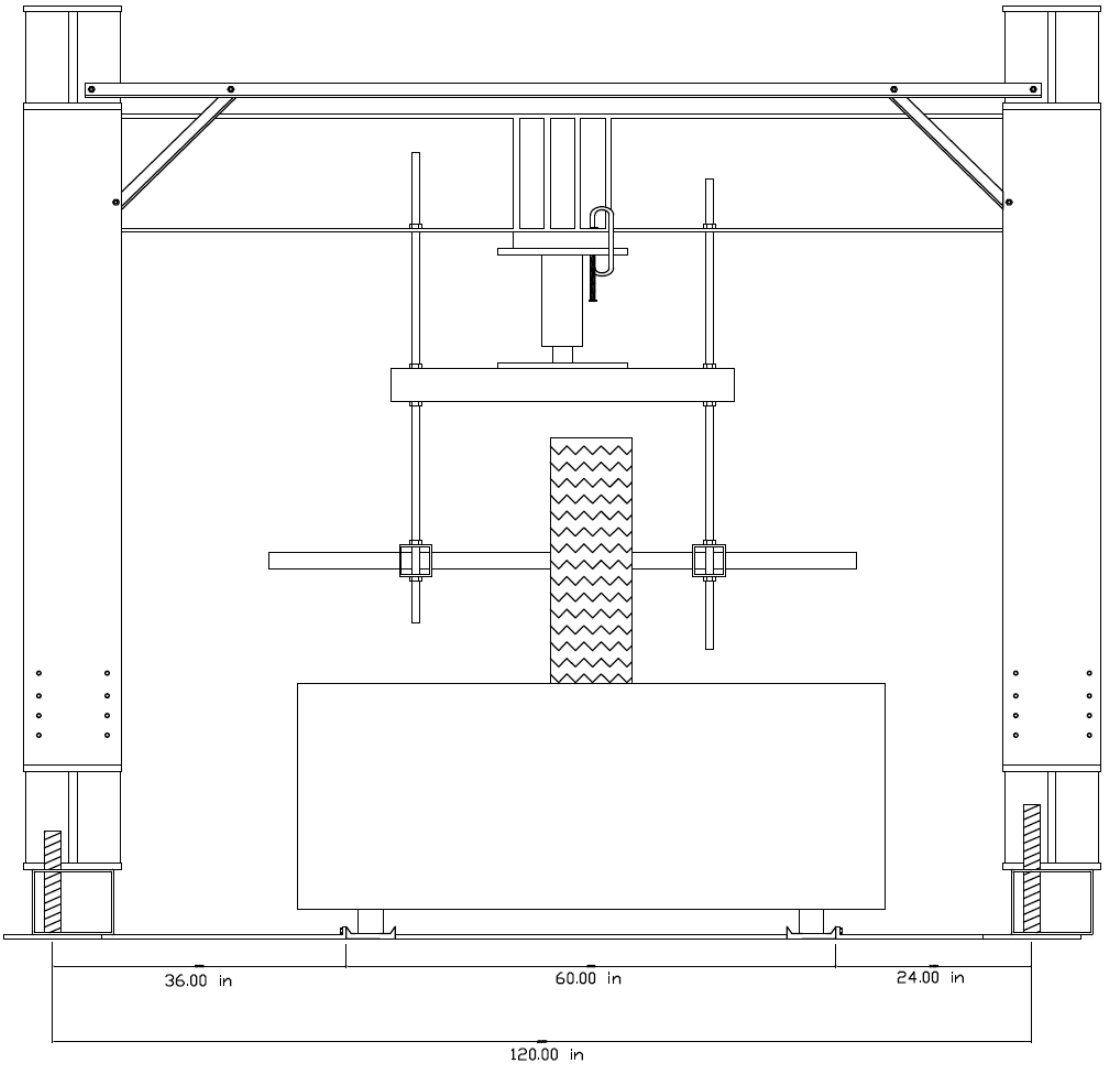
36.00 in
60.00 in
24.00 in
120.00 in

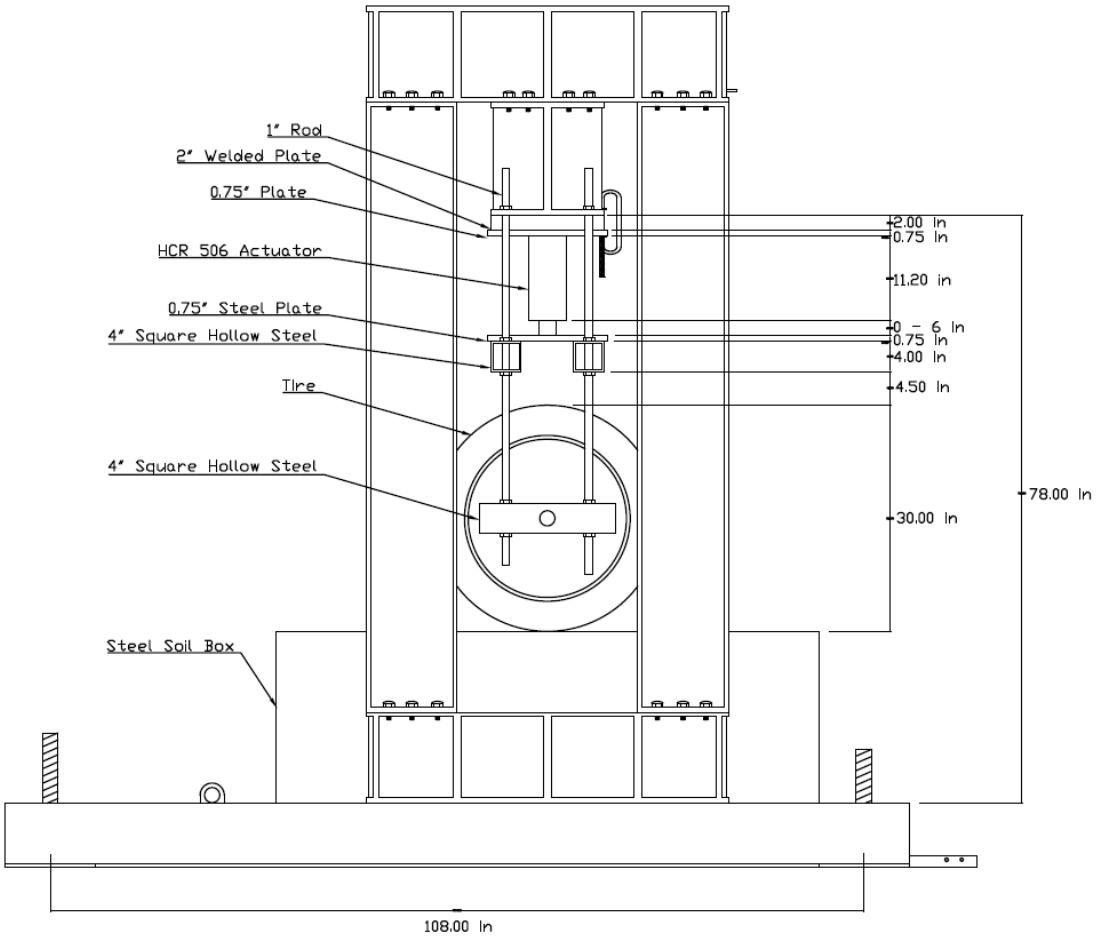
1" Rod
2" Welded Plate
0.75" Plate
HCR 506 Actuator
0.75" Steel Plate
4" Square Hollow Steel
Tire
4" Square Hollow Steel
Steel Soil Box
2.00 in
0.75 in
11.20 in
0 - 6 in
0.75 in
4.00 in
4.50 in
30.00 in
78.00 in
108.00 in

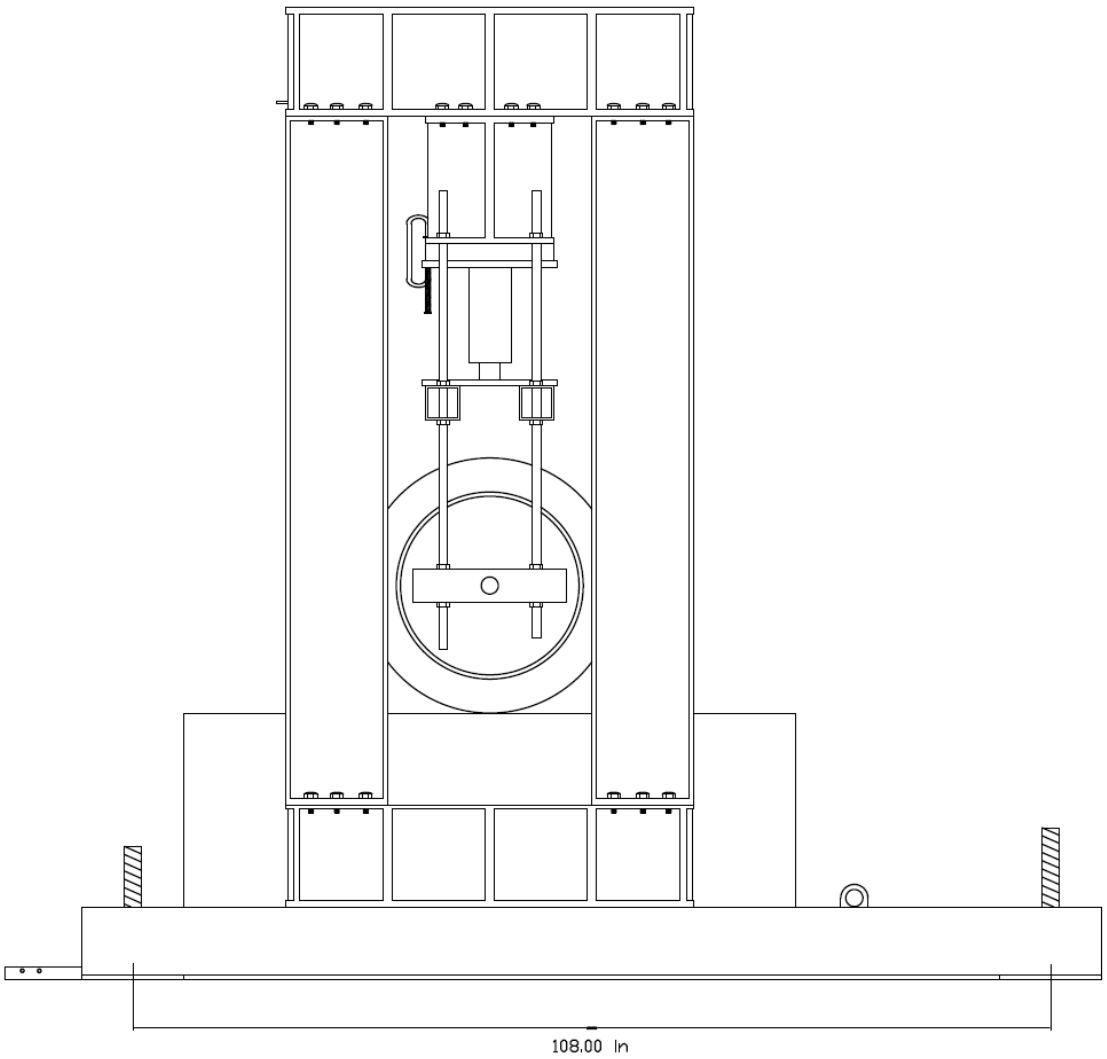
108.00 In

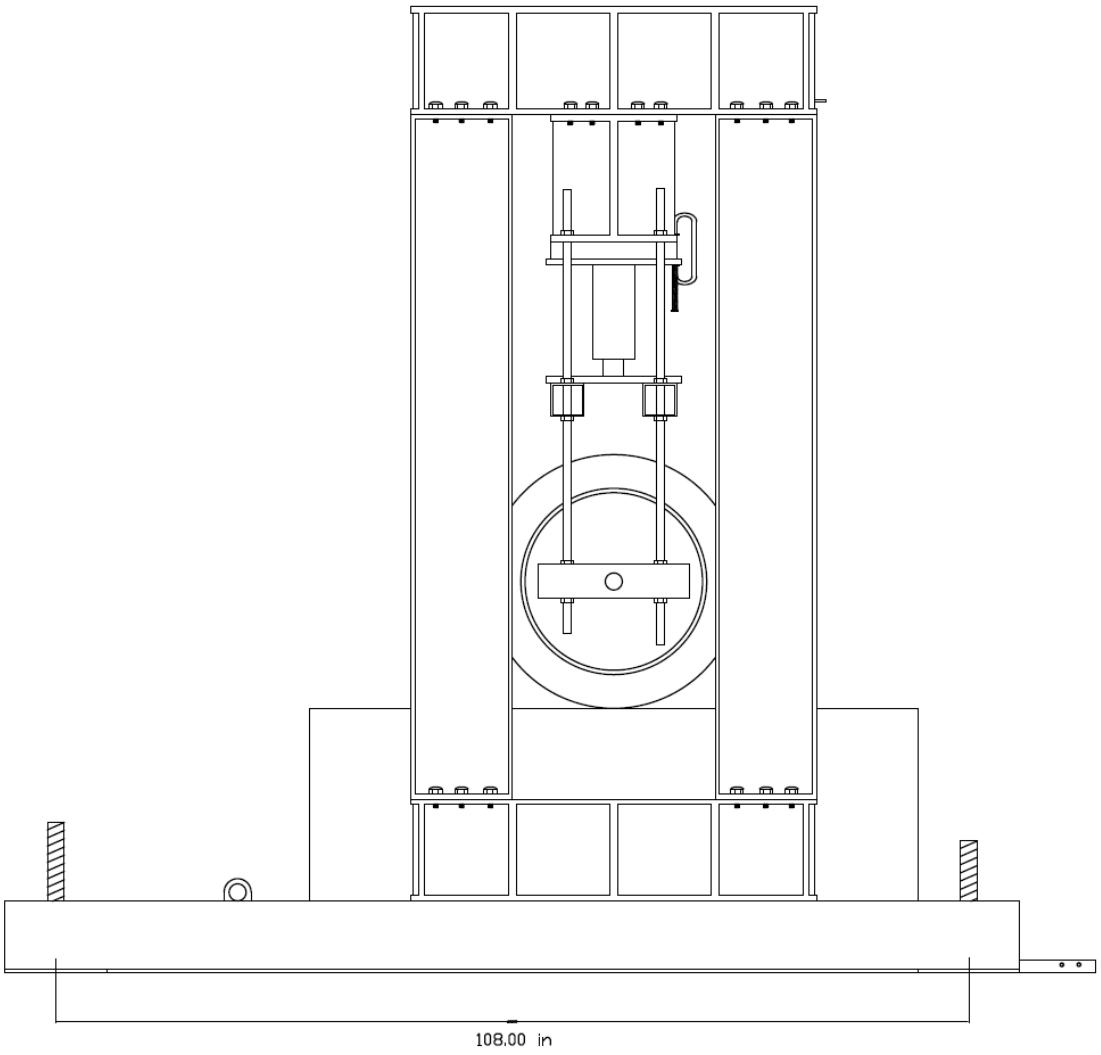
108.00 in

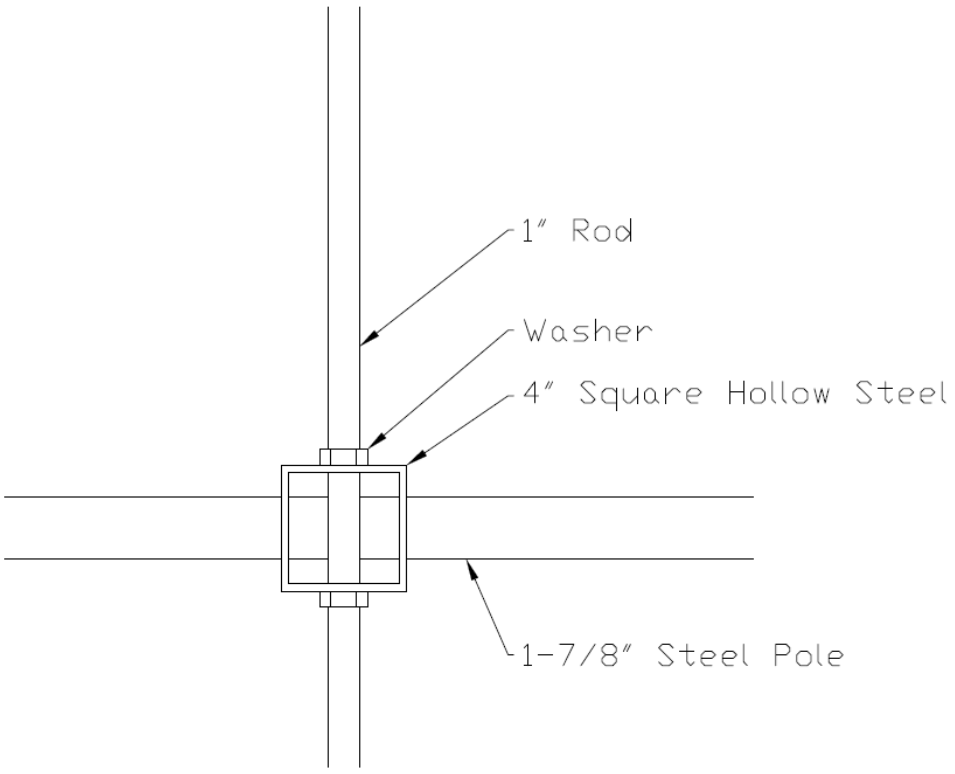

Callout A


108.00 in
36.00 in
60.00 in
24.00 in

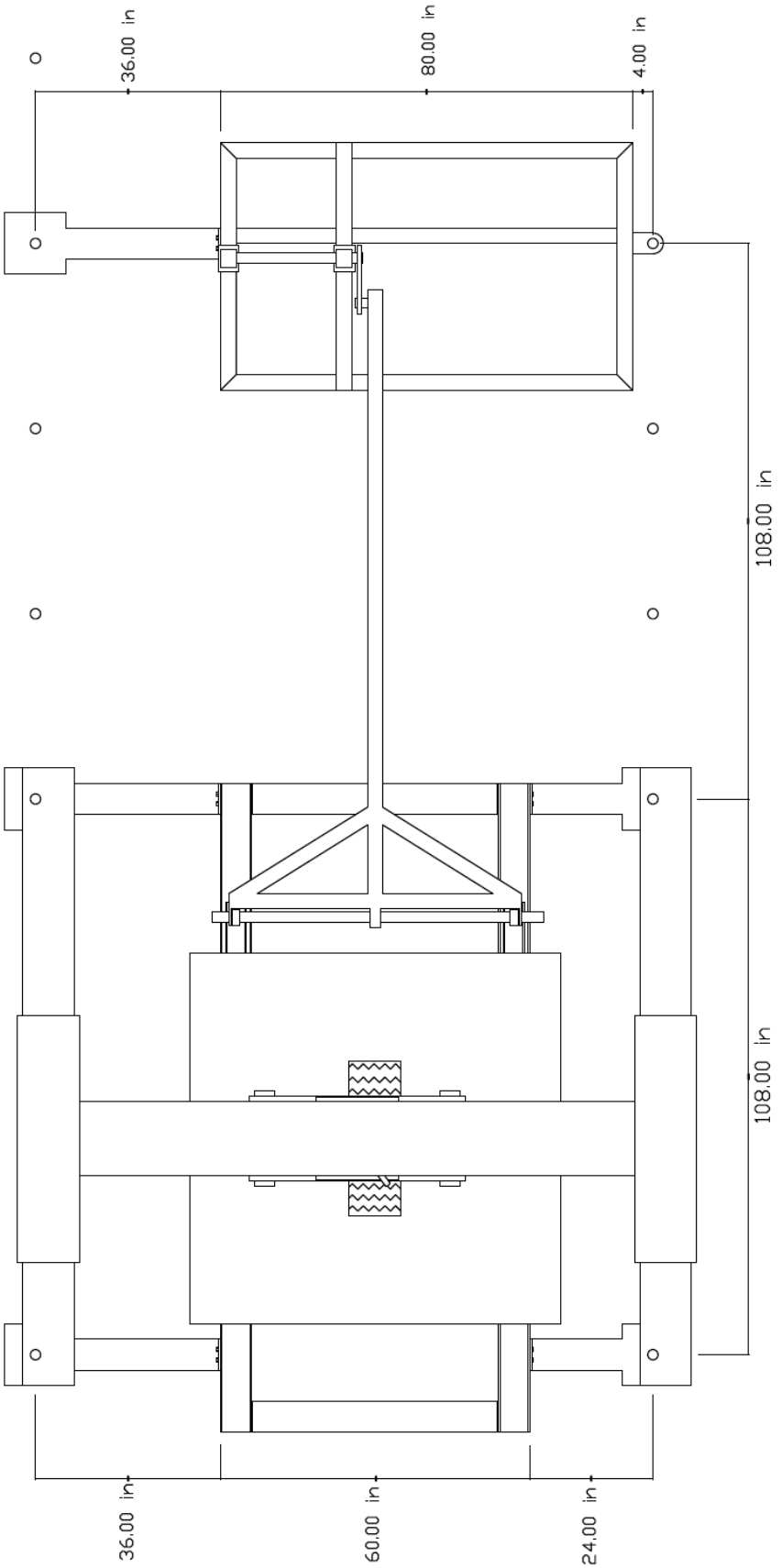
36.00 in
80.00 in
4.00 in
108.00 in
108.00 in
36.00 in
60.00 in
24.00 in

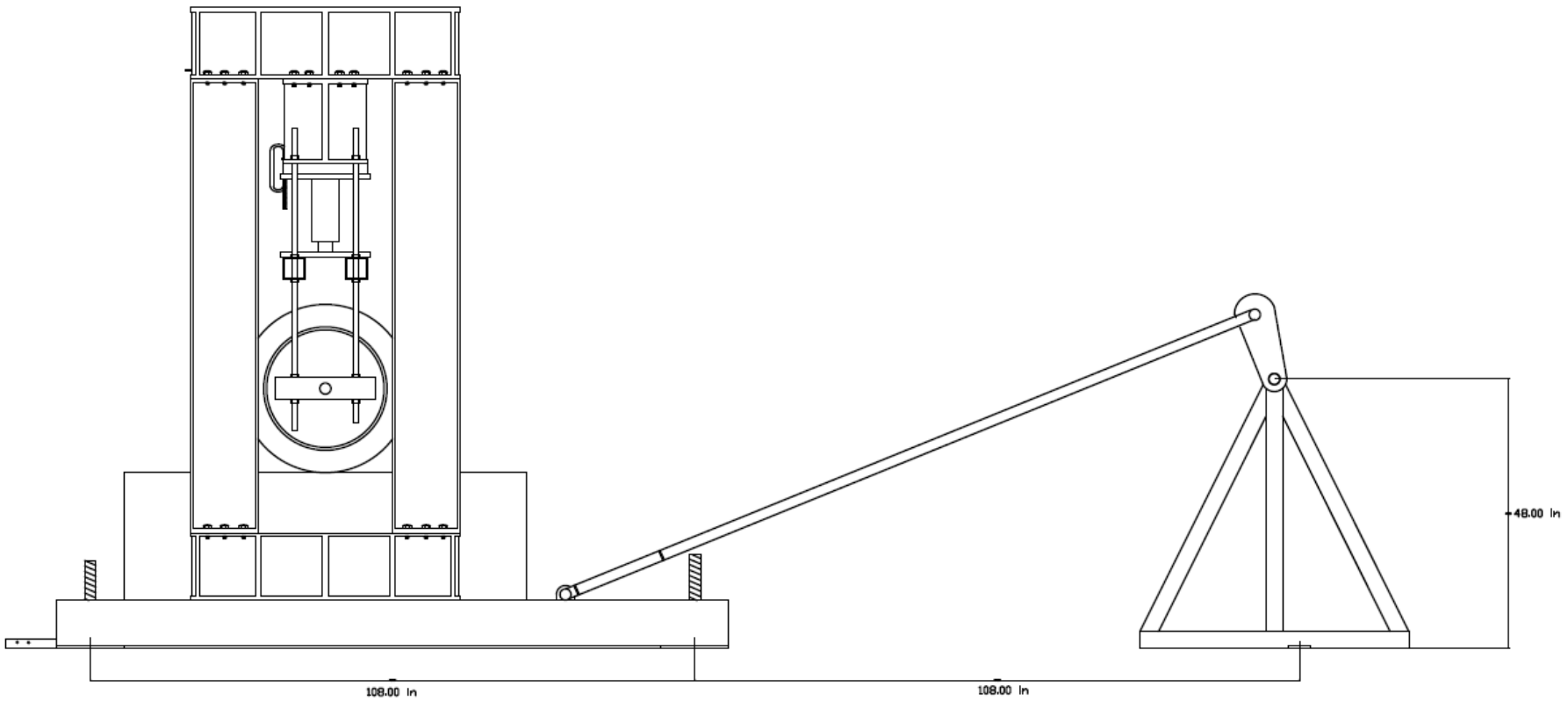
48.00 in
108.00 in
108.00 in